Targeting tyrosine hydroxylase for abdominal aortic aneurysm: impact on inflammation, oxidative stress and vascular remodelling

Laia Cañes[1,2,3], Judith Alonso[1,2,3], Carme Ballester-Servera[1,3], Saray Varona[1,2,3], José R Escudero[2,4], Vicente Andrés[2,6], Cristina Rodríguez[2,3,5,*] and José Martínez-González[1,2,3,*]

[1]Instituto de Investigaciones Biomédicas de Barcelona-Consejo Superior de Investigaciones Científicas (IIBB-CSIC), Barcelona, Spain.

[2]CIBER de Enfermedades Cardiovasculares, ISCIII, Madrid, Spain.

[3]Instituto de Investigación Biomédica Sant Pau, Barcelona, Spain.

[4] Servicios Mancomunados de Angiología, Cirugía Vascular y Endovascular, Hospitales de la Santa Creu i Sant Pau/Dos de Mayo, Barcelona, Spain.

[5]Institut de Recerca Hospital de la Santa Creu i Sant Pau (IRHSCSP), Barcelona, Spain.

[6]Centro Nacional de Investigaciones Cardiovasculares (CNIC), Madrid, Spain.

Short title: TH in abdominal aortic aneurysm.

Word count: 6676

Word count of the abstract: 249

Total number of figures: 6

[*]These authors contributed equally to this work. Correspondence should be addressed to J.M.-G. IIBB, Rosselló, 161, 08036 Barcelona, Spain (email: jose.martinez@iibb.csic.es; phone: +34 93 5565896) or C.R. IRHSCSP, C/Antoni Mª Claret, 08025 Barcelona, Spain (email: crodriguezs@santpau.cat; phone: +34 93 5565897).

Abstract

Pharmacological treatments for preventing abdominal aortic aneurysm (AAA) rupture or slowing aneurysm progression remain a challenge. It is increasingly recognized that sympathetic activity might play a role in the pathogenesis of AAA; however, the impact of this pathway remains unclear. Here, we show that the expression of tyrosine hydroxylase [*TH*], dopamine β-hydroxylase [*DBH*] and the norepinephrine transporter *SLC6A2* is upregulated in abdominal aorta samples from AAA patients and in the aneurysmal aorta from two animal models susceptible to angiotensin II (AngII)-induced AAA: the apolipoprotein E-deficient ($ApoE^{-/-}$) model and a transgenic mouse that over-expresses the human nuclear receptor NOR-1 (Neuron-derived orphan receptor-1) in the vascular wall ($TgNOR\text{-}1^{VSMC}$). TH localises to sympathetic nerves innervating the local vasculature, but also to inflammatory cells, and scattered VSMC in human and mouse AAA. Interestingly, the preventive effect of doxycycline on AAA formation in AngII-treated $TgNOR\text{-}1^{VSMC}$ mice was associated to the normalisation of vascular *Th* expression. Moreover, the TH specific inhibitor α-methyl-*p*-tyrosine protected against AngII-induced AAA formation, limiting the progressive increase in aortic diameter without affecting blood pressure. The drug normalised MMP2 expression and MMP activity, preserving elastin integrity, attenuated the AngII-mediated rise in vascular oxidative stress and inflammatory markers and reduced the inflammatory infiltrate. Finally, NOR-1, whose expression correlated with that of *TH* in human AAA, was able to drive human *TH* transcriptional activity in transient transfection assays. Therefore, the upregulation of the TH pathway could be critical in the pathophysiology of AAA, supporting the potential of pharmacological strategies targeting TH for AAA management.

Key words: abdominal aortic aneurysm, tyrosine hydroxylase, AMPT, animal models, NOR-1.

Introduction

Abdominal aortic aneurysm (AAA) is a common and life-threatening disorder affecting approximately 4% to 8% of men over 65 years of age.[1] It is characterized by a focal and permanent dilation of the abdominal aorta, whose diameter progressively grows increasing the risk of aortic rupture, a devastating condition responsible for more than 16,000 deaths each year in the United States alone.[2] In this disease, the arterial wall suffers a chronic inflammatory stage with upregulation of proteinases, that degrade structural matrix proteins, and loss of vascular smooth muscle cells (VSMC), which leads to a destructive remodelling of the arterial wall. Despite the high prevalence of AAA, surgical repair of those more severe is currently the only effective way to treat the disease. Nowadays, pharmacological treatments for preventing aortic rupture or slowing aneurysm progression remains a challenge.[3] Therefore, it is mandatory to identify novel therapeutic strategies for the medical management of this disease.

The sympathetic nervous system is key in cardiovascular homeostasis. Alterations in sympathetic function impacts on cardiovascular diseases such as hypertension, heart failure and myocardial infarction;[4] however, little is known about its role on AAA. In the last years, it is increasingly recognized that sympathetic activity might actively contribute to aneurysm progression and rupture. In fact, human aortic dissection is frequently associated with an increase in sympathetic activity,[5] while local sympathetic denervation ameliorates experimental aneurysms.[6] Recently, using a new mouse model that overexpresses the neuron-derived orphan receptor-1 (NOR-1) in the vascular wall[7] and recapitulates key aspects of human AAA, we suggested the upregulation of genes associated to sympathetic activity in aneurysmal aorta.[8] They include key components of the tyrosine hydroxylase (TH) pathway involved in the biosynthesis of catecholamines, important hormones and neurotransmitters in both the central and peripheral nervous systems.[9] The biological functions of the TH

pathway, however, are far from limited to the well-known effects of catecholamines on their main target tissues. Early studies showed that the inactivation of both TH alleles results in mid-gestational lethality, apparently due to cardiovascular failure.[10] More recently, it has been shown that the expression of TH during heart development is required to drive cells to a sino-atrial fate, the hallmark of cardiac chamber formation.[11] The TH pathway also appears to be critical modulating the pancreatic endocrine precursor and insulin producing cell neogenesis,[12] as well as lymphocyte differentiation and function, thereby controlling immune homeostasis.[13] This multiplicity of functions would explain the reason for the intricate mechanisms that regulate TH,[14] the first and rate-limiting step of the pathway, and the interest in this enzyme as a therapeutic target for human disease.[15] Here, we have addressed whether TH could actively contribute to AAA progression. Our data uncover the striking upregulation of the TH pathway in human AAA, and provide evidence that the inhibition of TH ameliorates AAA development in two experimental models of this disease. Altogether, these data support the interest of pharmacological strategies targeting TH for the clinical management of AAA.

Materials and methods

Detailed methods are provided in the Data Supplement. The data that support the findings of this study are available from the corresponding author upon reasonable request.

Aneurysm and donor sampling and preservation

Human abdominal aortic samples from patients undergoing open repair surgery for AAA at the Hospital de la Santa Creu i Sant Pau (HSCSP; Barcelona, Spain) and healthy specimens from multi-organ donors were obtained after signed informed consent, as described.[16,17]

Animal handling

The apolipoprotein E-deficient ($ApoE^{-/-}$) mice (Charles River Ltd; Kent, UK) and a mouse model that specifically over-expresses the human nuclear receptor NOR-1 in the vascular wall ($TgNOR\text{-}1^{VSMC}$)[7,18] were used. AAA was induced by angiotensin II (AngII), as reported.[8,19] AngII-infused mice were pre-treated with a tyrosine hydroxylase inhibitor (α-methyl-*p*-tyrosine [AMPT; Sigma-Aldrich]; 100 mg/Kg twice daily, i.p). Abdominal aorta diameter was measured by ultrasonography.[8,16,19,20] Abdominal aorta samples were processed for histological, immunohistochemical and expression analysis and for the assessment of $O_2^{\cdot -}$ production and MMP activity.[8,18,19,21]

Statistical Analyses

Results are shown as mean ± standard error of the mean (SEM). Significant differences ($p<0.05$) were analysed with the GraphPad Prism version 6.01, using one-way ANOVA, two-way ANOVA with repeated measures or two-way ANOVA and the Tukey's tests. When normality failed, the Mann–Whitney rank sum test or the Kruskal–Wallis test was applied. Differences in AAA incidence were analysed by the Chi square test ($\chi 2$) and the association between variables by the Pearson Product Moment Correlation method after Log_{10} data transformation.

Results

The catecholamine biosynthetic pathway is upregulated in human AAA

Recent results from high-throughput microarray expression studies in a preclinical model suggest the upregulation of genes related to sympathetic activity in aneurysmal tissues.[8] As shown in Figure 1A, the expression of genes encoding for enzymes of the TH pathway such as *TH* and dopamine β-hydroxylase (*DBH*), and the norepinephrine transporter *SLC6A2* was

increased in abdominal aorta samples from AAA patients compared with healthy donors. Clinical data from patients and donors are shown in Table S1. In particular, the expression of *TH*, the rate-limiting enzyme in this pathway, was strongly up-regulated in human aneurysmal tissue. Likewise, TH protein levels were consistently increased in a representative group of human AAA samples (Figure 1B, Table S2). Further, immunohistochemical analysis detected TH in areas of vascular innervations and in inflammatory cells, whereas scattered TH-positive vascular smooth muscle cells (VSMC) could be found in media (Figure 1C, upper and middle panels). TH immunostaining was hardly detected in abdominal aorta from healthy donors (Figure 1C, lower panel).

Increased TH expression in mouse models of AAA

We addressed whether the catecholamine biosynthetic pathway is also upregulated in experimental AAA. Real-time PCR revealed increased expression of *Th*, *Dbh*, dopa decarboxylase (*Ddc*), and *Scl6a2* in AngII-induced AAA from $ApoE^{-/-}$ (Figure 2A). Interestingly, the over-expression of these genes was observed few days after AngII infusion, before AAA is formed (Figure S1). The TH pathway was also upregulated in AngII-induced AAA from TgNOR-1^{VSMC} mice[8] (Figure S2A), and a concomitant increase of TH protein levels was manifest in diseased aortas from both animal models (Figure 2B and Figure S2B). The upregulation of aortic TH expression by AngII was more evident in the mouse strain sensitive to AAA than in wild-type (WT) animals (Figure S3). The immunohistochemical expression pattern of TH in aneurysmal aortas from both mouse models was similar to that observed in AAA from patients, namely a pronounced staining in vascular innervations and inflammatory cells and, to a lesser extent, in VSMC (Figure 2C, Figure S2C). Therefore, the vascular upregulation of TH is a common feature of the aneurysmal disease in both humans and animal models.

The increase in TH activity contributes to AAA development in the AngII-infused ApoE$^{-/-}$ model.

We have previously shown the effectiveness of doxycycline to prevent the formation of AAA induced by AngII in TgNOR-1^{VSMC} mice.[8] As shown in Figure S4, this doxycycline effect is associated with the normalisation of *Th* expression. This prompted us to determine whether the up-regulation of vascular TH might play an active role in AAA pathophysiology. For this purpose, α-methyl-*p*-tyrosine (AMPT), a specific inhibitor of TH, was administered to AngII-infused ApoE$^{-/-}$ mice (100 mg/Kg twice daily). This AMPT dosage regimen normalised plasma noradrenaline levels in animals infused with AngII (Figure S5). Interestingly, AMPT protected against AAA formation limiting the progressive increase in aortic diameter evoked by AngII (Figure 3A-C). While 80% of ApoE$^{-/-}$ mice infused with AngII developed aneurysms, AMPT substantially reduced this percentage to less than 10%, and avoided the development of the most severe forms of AAA (Figure 3D). Image analysis of histological sections confirmed the ultrasonographic findings (Figure S6). A slight improvement in the survival rate was detected in AMPT-treated mice although it did not reach statistical significance (Figure S7A). The impact of AMPT was independent of hemodynamic effects, since this drug did not affect blood pressure (Figure 3E). Neither body weight nor plasma lipid profile was modified by this intervention (Table S3). Likewise, AMPT did not alter circulating levels of aspartate and alanine transaminases or those of creatinine in AngII-infused ApoE$^{-/-}$ mice, while normalised blood urea nitrogen (BUN) levels (Figure S8A). Concerning vascular phenotype, AngII-infused ApoE$^{-/-}$ mice subjected to AMPT treatment recapitulated most features of saline-infused animals (Figure 3F), preserving elastin integrity associated with normalised vascular metalloproteinase-2 (MMP2) expression and MMP activity (Figure 4A-C and Figure S9). Further, AMPT decreased the vascular expression of

inflammatory markers such as *Emr1* and *Mcp1* (Figure 4C), and the recruitment of macrophages, lymphocytes and neutrophils into the vessel wall (Figure S9 and S10A). Likewise, AMPT attenuated the rise in vascular oxidative stress induced by AngII (Figure 4D). These vascular effects were associated to the downregulation of TH in AMPT-treated animals (Figure S11A-B).

The increase in TH activity contributes to the enhanced susceptibility of TgNOR-1^{VSMC} mice to AAA

AMPT also protected against AAA formation in the AngII-infused TgNOR-1^{VSMC} mouse model, an effect that reached statistical significance at day 14 (Figure 5A-C). This drug reduced the aneurysm incidence and severity (Figure 5D). AMPT neither affected blood pressure (Figure 5E) nor body weight (not shown), but normalised BUN levels (Figure S8B). As previously reported,[8] Ang-II infusion led to the early death of about 20% of animals, effect slightly attenuated by AMPT although without statistical significance (Figure S7B). Further, AMPT ameliorated vascular remodelling (Figure 5F) and elastin fibre disruption in challenged NOR-1 transgenic mice (Figure 6A). Concomitantly, in AMPT-treated animals, both MMP2 expression and MMP activity were comparable to that of control animals (Figure 6B-C and Figure S12). Similarly, AMPT completely prevented the increase in the vascular expression of inflammatory markers (*Emr1*, *Mcp1*, *Il1β*, *Il6* and *Cxcl2*) (Figure 6C) and the infiltration of inflammatory cells induced by AngII (Figure S12 and S10B). TH inhibition also avoided the enhanced vascular generation of $O_2^{\cdot -}$ (Figure 6D) evoked by AngII. These AMPT effects were associated to the downregulation of TH (Figure S11C-D).

NOR-1 modulates human *TH* expression in VSMC

Interestingly, in human aneurysms we found a significant correlation between *NOR-1* expression and that of *TH* (Figure S13). Since *TH* has been shown to be regulated by Nurr1 (NR4A2) in non-vascular cells,[22] we addressed whether NOR-1 (NR4A3) could directly modulate *TH* expression. *In silico* analysis of human *TH* proximal promoter identified a putative NBRE site (Figure S14A). Transient cotransfection of VSMC with a *TH* promoter-driven luciferase reporter construct and a NOR-1 expression vector evidenced that NOR-1 overexpression significantly increased *TH* transcriptional activity (Figure S14B). Further, site-directed mutagenesis revealed the major contribution of this NBRE site to the NOR-1-dependent *TH* regulation (Figure S14B and Table S4). In agreement, NOR-1 expression was early induced by AngII in vascular cells (Figure S14C). Taken together, these results suggest that NOR-1 could be one of the transcription factors involved in the regulation of TH in the vasculature.

Discussion

The lack of pharmacological approaches is a great handicap for the management of AAA, and patients live for years under the sword of Damocles fearing a fatal rupture. Here we uncover an instrumental role of the TH pathway on the pathophysiology of this disease, and suggest the rate-limiting enzyme TH as a potential pharmacological target.

Our data evidence that genes encoding for proteins involved in the TH pathway and the transport of norepinephrine are upregulated in human aneurysmal samples. Previous gene expression microarray studies suggested that gene pathways related to neuronal activity are enriched in human AAA.[23] In that study, however, the regulation of genes of the TH pathway did not reach statistical significance. Recently, data from a whole genome-expression profiling analysis of aortic tissues from AngII-infused TgNOR-1^{VSMC} mice evidenced that AAA are enriched in gene sets related to sympathetic activation.[8] Here, we confirm (by real-

time PCR) and expand these observations in two mouse models prone to AngII-induced aortic aneurysm, the ApoE knockout mouse and a NOR-1 transgenic mouse. In particular, we ascertain that the expression of TH is strongly induced in aneurysmal lesions from both humans and animal models. Noteworthy, the increase in vascular TH expression triggered by AngII in both mouse models is in line with previous data reporting the upregulation of TH by this peptide hormone in other tissues.[24] These data suggested that TH activity could play an active role in AAA and in the ability of AngII to promote aneurysm formation.

Different evidences suggest that catecholamines critically influence vascular remodelling. Indeed, sympathetic hyperactivity underlies the pathophysiology of aortopathies such thoracic aortic dissection (TAD),[5,25] and both sympathetic hyperactivity and aortic sympathetic nerve sprouting have been documented in patients with TAD.[5] Further, AngII, a key player in AAA formation,[26] enhances sympathetic activity inducing aortic MMP2, which plays a critical role in the onset and progression of several aortopathies including AAA.[27] Moreover, Hu *et al*.[6] showed that catecholamines regulate TGFβ signalling in aortic aneurysms, limiting VSMC proliferation and fostering apoptosis, thereby modulating vascular remodelling. Interestingly, the TH pathway has been previously documented in the vascular wall, and TH expression has been demonstrated in VSMC, endothelial cells and regulatory T cells.[13,28-30] In agreement, our studies in human and mouse aneurysms detected TH immunostaining localised to vascular innervations but also to inflammatory cells and VSMC. Interestingly, we observe that the effectiveness of doxycycline to prevent the formation of AAA induced by AngII in TgNOR-1^{VSMC} mice[8] is associated with the normalisation of vascular *Th* expression. Doxycycline is a MMP inhibitor, able to exert a number of potentially beneficial cellular effects,[31,32] which prevents the formation of experimental AAA in animal models,[33] and reduced vascular inflammation in clinical trials.[34] The unanticipated downregulation of *Th* expression by doxycycline requires further

investigation and suggest the active involvement of TH in AAA, but its potential as a therapeutic target had not been explored.

In light of these data, we tested the efficacy of TH blockade limiting AAA growth. AngII-infused ApoE$^{-/-}$ and TgNOR-1^{VSMC} mice were treated with AMPT, an orally available and well-tolerated competitive inhibitor of TH, which blocks catecholamine biosynthesis.[35] This drug was administered at a dosage regimen that assured an effective inhibition of the enzyme.[36] Notably, under these conditions, AMPT largely protected from AngII-induced AAA in both experimental models. In the clinical setting, AMPT has only been approved for the control of hypertension and other symptoms associated with the excess of catecholamines produced by pheochromocytoma.[37] Further, this drug has also been proposed for the management of movement disorders and some neuropsychiatric diseases.[38] In patients with pheochromocytoma, AMPT limits the hypertensive response evoked by the catecholamine-producing tumour; however, no beneficial effect has been recognized for this drug on essential hypertension.[38] Similarly, in our hands AMPT did not affect blood pressure. Thus, targeting TH, this drug prevents AngII-induced AAA, which has previously been shown to be largely independent of the AngII vasopressor function.[39] AMPT not only limited aortic diameter expansion, but also inflammation and vascular oxidative stress and preserved vascular wall integrity. TH activity has been associated with the generation of reactive oxygen species (ROS) and oxidative stress,[40] and inflammation.[41] Accordingly, in experimental models of AAA, we found that AMPT significantly attenuated vascular oxidative stress, reduced the immune infiltrate and improved the expression profile of proinflammatory cytokines, thus suggesting that TH upregulation could account, at least in part, for the pathophysiology of AAA. Consistently, previous reports have suggested that AMPT ameliorates oxidative stress and inflammation in other pathological settings.[42,43] Noteworthy, these vascular effects were associated to the downregulation of TH in AMPT

treated animals. Therefore, our data indicate that TH upregulation negatively impacts on AAA formation and support the potential of targeting this enzyme in AAA. DBH or SLC6A2, which were upregulated in AAA as well, could also be regarded as potential targets for this disease. However, TH inhibition results in an overall reduction of catecholamines and their metabolites,[44] which cannot be achieved by blocking DBH or SLC6A2, and, therefore, it is difficult to anticipate the impact of such blockade on aneurysm formation. For the same reason, TH inhibition leads to a biological scenario not equivalent to that of β-blockers. Finally, it should be highlighted that AMPT exerted its benefits on aneurysm formation in the absence of deleterious effects on other organs. For instance, blood creatinine levels were neither affected by AngII infusion nor by AMPT suggesting that our experimental conditions did not significantly affect renal function. In agreement, the renal expression of neutrophil gelatinase-associated lipocalin (*Ngal*) or Tenascin C (*Tnc*) remained unchanged in mice infused with AngII (both in the presence or absence of AMPT) (Figure S15). Although AMPT attenuated the slight increase in BUN levels produced by AngII infusion, our data do not allow attributing a relevant effect of this drug on renal function. Further studies in animal models more sensitive to kidney damage should be undertaken to analyze whether prolonged administration of AMPT affects renal function.

The regulation of TH expression is complex and cell type-specific.[22] Previous studies in non-vascular tissues identified *TH* as a target gene for the nuclear receptor Nurr1 (NR4A2). Surprisingly, Nurr1 transactivates or represses *TH* transcription (depending on cell-type).[45,46] Whether other members of the NR4A family, and specifically NOR-1 (NR4A3), that is upregulated in human AAA and contributes to vascular remodelling,[47] could also target *TH* is uncertain. We show that, in human AAA, NOR-1 expression significantly correlates with that of *TH*. Further, by transient transfection assays we identified one NBRE site responsible for the transcriptional regulation of human *TH* by NOR-1. Interestingly,

despite the human *TH* promoter show low homology with *TH* promoters from other species, this NBRE site is conserved among species (Figure S16).[48] It has been previously shown that AngII is able to modulate TH expression in several tissues.[49,50] Further, separate studies have documented the upregulation of NOR-1 by AngII both in vascular and non-vascular cells.[51,52] Our results indicate that NOR-1 could be involved in the upregulation of TH in humans AAA as well as in the vasculature of animals prone to develop AAA in response to AngII, and suggest a relevant role of this nuclear receptor in the pathogenesis of AAA.

Finally, interestingly enough, several case reports have described the coexistence of pheochromocytoma and other neuroendocrine tumours with aortic dissections and aneurysm rupture supporting that TH pathway hyperactivity might contribute to aneurysm development and eventually aortic rupture in these patients.[53-54] Further, high TH and both overall and regional aortic sympathetic nervous system activities have been documented in patients with TAD.[5] Our study evidences for the first time, that the upregulation of the TH pathway could be critical in the pathophysiology of AAA, both in humans and animal experimental models, and supports the therapeutic potential of approaches based on targeting this pathway for the medical management of AAA.

Perspectives

AAA is a life-threatening disorder; however pharmacological treatments preventing aortic rupture or slowing aneurysm progression are not available. Therefore, the identification of novel therapeutic strategies for the medical management of this disease remains a major challenge that requires an improved knowledge about the underlying molecular mechanisms. Sympathetic overactivation arises as a pivotal player in aneurysmal disease and our results support that targeting TH may represent a valuable therapeutic approach to hamper AAA development. Further research is warranted to develop optimised TH inhibitors featuring

improved pharmacokinetic characteristics and avoiding central side-effects due to dopamine depletion reported in AMPT-treated patients.

Acknowledgements

We thank Silvia Aguiló, Joan Repullés and Cristina González for their technical assistance.

Sources of funding

This work was supported by the Spanish Ministerio de Ciencia e Innovación (RTI2018-094727-B-100 and PID2019-108489RB-100), Instituto de Salud Carlos III (ISCIII) (PI18/0919), the Agència de Gestió d'Ajuts Universitaris i de Recerca (AGAUR) (2017-SGR-00333), and Sociedad Española de Arteriosclerosis (SEA-2019). The study was co-founded by Fondo Europeo de Desarrollo Regional (FEDER), a way to make Europe. L.C. and C.B-S were supported by a FI (AGAUR) and a FPU fellowship (Ministerio de Universidades), respectively.

Disclosures

None.

References

1. Nordon IM, Hinchliffe RJ, Loftus IM, Thompson MM. Pathophysiology and epidemiology of abdominal aortic aneurysms. *Nat Rev Cardiol*. 2011;8:92-102.
2. Mozaffarian D, Benjamin EJ, Go AS, Arnett DK, Blaha MJ, Cushman M, de Ferranti S, Després JP, Fullerton HJ, Howard VJ, et al. Heart disease and stroke statistics–2015 update: a report from the American Heart Association. Circulation. 2015;131:e29–322.

3. Golledge J. Abdominal aortic aneurysm: update on pathogenesis and medical treatments. *Nat Rev Cardiol*. 2019;16:225-242.

4. Grassi G, Seravalle G, Mancia G. Sympathetic activation in cardiovascular disease: evidence, clinical impact and therapeutic implications. *Eur J Clin Invest*. 2015; 45:1367-75.

5. Zhipeng H, Zhiwei W, Lilei Y, Hao Z, Hongbing W, Zongli R, Hao C, Xiaoping H. Sympathetic hyperactivity and aortic sympathetic nerve sprouting in patients with thoracic aortic dissection. *Ann Vasc Surg.* 2014;28:1243-1248.

6. Hu Z, Li B, Wang Z, Hu X, Zhang M, Chen R, Wu Q, Jia F. The sympathetic transmitter norepinephrine inhibits VSMC proliferation induced by TGFβ by suppressing the expression of the TGFβ receptor ALK5 in aorta remodelling. *Mol Med Rep*. 2020;22:387-397.

7. Rodríguez-Calvo R, Guadall A, Calvayrac O, Navarro MA, Alonso J, Ferrán B, de Diego A, Muniesa P, Osada J, Rodríguez C, et al. Over-expression of neuron-derived orphan receptor-1 (NOR-1) exacerbates neointimal hyperplasia after vascular injury. *Hum Mol Genet*. 2013;22:1949-1959.

8. Cañes L, Martí-Pàmies I, Ballester-Servera C, Alonso J, Serrano E, Briones AM, Rodríguez C, Martínez-González J. High neuron derived orphan receptor-1 (NOR-1) expression strengthens the vascular wall response to angiotensin II leading to aneurysm formation in mice. *Hypertension*. 2021;77:557-570.

9. Tank AW, Lee Wong D. Peripheral and central effects of circulating catecholamines. *Compr Physiol*. 2015;5:1-15.

10. Zhou QY, Quaife CJ, Palmiter RD. Targeted disruption of the tyrosine hydroxylase gene reveals that catecholamines are required for mouse fetal development. *Nature*. 1995;374:640-643.

11. López-Sánchez C, Bártulos O, Martínez-Campos E, Gañán C, Valenciano AI, García-Martínez V, De Pablo F, Hernández-Sánchez C. Tyrosine hydroxylase is expressed during

early heart development and is required for cardiac chamber formation. *Cardiovasc Res*. 2010;88:111-120.

12. Vázquez P, Robles AM, de Pablo F, Hernández-Sánchez C. Non-neural tyrosine hydroxylase, via modulation of endocrine pancreatic precursors, is required for normal development of beta cells in the mouse pancreas. *Diabetologia*. 2014;57:2339-2347.
13. Cosentino M, Fietta AM, Ferrari M, Rasini E, Bombelli R, Carcano E, Saporiti F, Meloni F, Marino F, Lecchini S Human CD4+CD25+ regulatory T cells selectively express tyrosine hydroxylase and contain endogenous catecholamines subserving an autocrine/paracrine inhibitory functional loop. *Blood*. 2007;109:632-642.
14. Lenartowski R, Goc A. Epigenetic, transcriptional and posttranscriptional regulation of the tyrosine hydroxylase gene. *Int J Dev Neurosci*. 2011;29:873-883.
15. Waløen K, Kleppe R, Martinez A, Haavik J. Tyrosine and tryptophan hydroxylases as therapeutic targets in human disease. *Expert Opin Ther Targets*. 2017;21:167-180.
16. Orriols M, Varona S, Martí-Pàmies I, Galán M, Guadall A, Escudero JR, Martín-Ventura JL, Camacho M, Vila L, Martínez-González J, et al. Down-regulation of Fibulin-5 is associated with aortic dilation: role of inflammation and epigenetics. *Cardiovasc Res*. 2016;110:431-442.
17. Alonso J, Galán M, Martí-Pàmies I, Romero JM, Camacho M, Rodríguez C, Martínez-González J. NOR-1/NR4A3 regulates the cellular inhibitor of apoptosis 2 (cIAP2) in vascular cells: role in the survival response to hypoxic stress. *Sci Rep*. 2016;6:34056.
18. Cañes L, Martí-Pàmies I, Ballester-Servera C, Herraiz-Martínez A, Alonso J, Galán M, Nistal JF, Muniesa P, Osada J, Hove-Madsen L, et al. Neuron-derived orphan receptor-1 modulates cardiac gene expression and exacerbates angiotensin II-induced cardiac hypertrophy. *Clin Sci (Lond)*. 2020;134:359-377.

19. Galán M, Varona S, Orriols M, Rodríguez JA, Aguiló S, Dilmé J, Camacho M, Martínez-González J, Rodriguez C. Induction of histone deacetylases (HDACs) in human abdominal aortic aneurysm: therapeutic potential of HDAC inhibitors. *Dis Model Mech*. 2016;9:541-552.

20. Manning MW, Cassis LA, Daugherty A. Differential effects of doxycycline, a broad-spectrum matrix metalloproteinase inhibitor, on angiotensin II-induced atherosclerosis and abdominal aortic aneurysms. *Arterioscler Thromb Vasc Biol*. 2003;23:483-488.

21. Martínez-Revelles S, García-Redondo AB, Avendaño MS, Varona S, Palao T, Orriols M, Roque FR, Fortuño A, Touyz RM, Martínez-González J, et al. Lysyl oxidase induces vascular oxidative stress and contributes to arterial stiffness and abnormal elastin structure in hypertension: role of p38MAPK. *Antioxid Redox Signal*. 2017;27:379-397.

22. Kim TE, Park MJ, Choi EJ, Lee HS, Lee SH, Yoon SH, Oh CK, Lee BJ, Kim SU, Lee YS, et al. Cloning and cell type-specific regulation of the human tyrosine hydroxylase gene promoter. *Biochem Biophys Res Commun*. 2003;312:1123-1131.

23. Lenk GM, Tromp G, Weinsheimer S, Gatalica Z, Berguer R, Kuivaniemi H. Whole genome expression profiling reveals a significant role for immune function in human abdominal aortic aneurysms. *BMC Genomics.* 2007;8:237.

24. Dogan MD, Sumners C, Broxson CS, Clark N, Tümer N. Central angiotensin II increases biosynthesis of tyrosine hydroxylase in the rat adrenal medulla. *Biochem Biophys Res Commun*. 2004;313:623-626.

25. Hu R, Wang Z, Ren Z, Liu M. Autonomic remodelling may be responsible for decreased incidence of aortic dissection in STZ-induced diabetic rats via down-regulation of matrix metalloprotease 2. *BMC Cardiovasc Disord*. 2016;16:200.

26. Hackam DG, Thiruchelvam D, Redelmeier DA. Angiotensin-converting enzyme inhibitors and aortic rupture: a population-based case-control study. *Lancet*. 2006;368:659-665.

27. Hu Z, Wang Z, Wu H, Yang Z, Jiang W, Li L, Hu X. Ang II enhances noradrenaline release from sympathetic nerve endings thus contributing to the up-regulation of metalloprotease-2 in aortic dissection patients' aorta wall. *PLoS One*. 2013;8:e76922.

28. Pfeil U, Kuncova J, Brüggmann D, Paddenberg R, Rafiq A, Henrich M, Weigand MA, Schlüter KD, Mewe M, Middendorff R, et al. Intrinsic vascular dopamine - a key modulator of hypoxia-induced vasodilatation in splanchnic vessels. *J Physiol*. 2014;592:1745-1756.

29. Sorriento D, Santulli G, Del Giudice C, Anastasio A, Trimarco B, Iaccarino G. Endothelial cells are able to synthesize and release catecholamines both in vitro and in vivo. *Hypertension*. 2012;60:129-136.

30. Huang HW, Zuo C, Chen X, Peng YP, Qiu YH. Effect of tyrosine hydroxylase overexpression in lymphocytes on the differentiation and function of T helper cells. *Int J Mol Med*. 2016;38:635-642.

31. Chung AW, Yang HH, Radomski MW, van Breemen C. Long-term doxycycline is more effective than atenolol to prevent thoracic aortic aneurysm in marfan syndrome through the inhibition of matrix metalloproteinase-2 and -9. *Circ Res*. 2008;102:e73-85.

32. Hao L, Nishimura T, Wo H, Fernandez-Patron C. Vascular responses to alpha1-adrenergic receptors in small rat mesenteric arteries depend on mitochondrial reactive oxygen species. *Arterioscler Thromb Vasc Biol*. 2006;26:819-825.

33. Dodd BR, Spence RA. Doxycycline inhibition of abdominal aortic aneurysm growth – a systematic review of the literature. *Curr Vasc Pharmacol*. 2011;9:471-478.

34. Baxter BT, Matsumura J, Curci JA, McBride R, Larson L, Blackwelder W, Lam D, Wijesinha M, Terrin M; N-TA3CT Investigators. Effect of doxycycline on aneurysm growth among patients with small infrarenal abdominal aortic aneurysms: a randomized clinical trial. *JAMA*. 2020;323:2029-2038.

35. Brogden RN, Heel RC, Speight TM, Avery GS. α-Methyl-p-tyrosine: A review of its pharmacology and clinical use. *Drugs*. 1981;21:81-89.

36. Meltzer HY, Fessler RG, Simonovic M, Doherty J, Fang VS. Effect of d- and l-amphetamine on rat plasma prolactin levels. *Psychopharmacology (Berl).* 1979;61:63-69.

37. DEMSER (metyrosine) capsule. FDA prescribing information. Accessed October 31 2016. https://www.drugs.com/pro/demser.html.

38. Bloemen OJ, de Koning MB, E. Boot E, Booij J, van Amelsvoort TA. Challenge and therapeutic studies using alpha-methyl-para-tyrosine (AMPT) in neuropsychiatric disorders: a review. *Cent Nerv Syst Agents Med Chem*. 2008;8:249-256.

39. Cassis LA, Gupte M, Thayer S, Zhang X, Charnigo R, Howatt DA, Rateri DL, Daugherty A. ANG II infusion promotes abdominal aortic aneurysms independent of increased blood pressure in hypercholesterolemic mice. *Am J Physiol Heart Circ Physiol*. 2009;296:H1660-1665.

40. Meiser J, Weindl D, Hiller K. Complexity of dopamine metabolism. *Cell Commun Signal*. 2013;11:34.

41. Tolleson C, Claassen D. The function of tyrosine hydroxylase in the normal and Parkinsonian brain. *CNS Neurol Disord Drug Targets*. 2012;11:381-386.

42. Çimen O, Çimen FK, Gülaboğlu M, Bilgin AÖ, Çekiç AB, Eken H, Süleyman Z, Bilgin Y, Altuner D. The effect of metyrosine on oxidative gastric damage induced by ischemia/reperfusion in rats. Biochemical and histopathological evaluation. *Acta Cir Bras.* 2018;33:259-267.

43. Albayrak A, Polat B, Cadirci E, Hacimuftuoglu A, Halici Z, Gulapoglu M, Albayrak F, Suleyman H. Gastric anti-ulcerative and anti-inflammatory activity of metyrosine in rats. *Pharmacol Rep*. 2010;62:113-119.

44. Naruse M, Satoh F, Tanabe A, Okamoto T, Ichihara A, Tsuiki M, Katabami T, Nomura M, Tanaka T, Matsuda T, et al. Efficacy and safety of metyrosine in pheochromocytoma/paraganglioma: a multi-center trial in Japan. *Endocr J*. 2018;65:359-371

45. Kim KS, Kim CH, Hwang DY, Seo H, Chung S, Hong SJ, Lim JK, Anderson T, Isacson O. Orphan nuclear receptor Nurr1 directly transactivates the promoter activity of the tyrosine hydroxylase gene in a cell-specific manner. *J Neurochem*. 2003;85:622-634.

46. Kim TE, Seo JS, Yang JW, Kim MW, Kausar R, Joe E, Kim BY, Lee MA. Nurr1 represses tyrosine hydroxylase expression via SIRT1 in human neural stem cells. *PLoS One*. 2013;8:e71469.

47. Martínez-González J, Rius J, Castelló A, Cases-Langhoff C, Badimon L. Neuron-derived orphan receptor-1 (NOR-1) modulates vascular smooth muscle cell proliferation. *Circ Res*. 2003;92:96-103.

48. Kessler MA, Yang M, Gollomp KL, Jin H, Iacovitti L. The human tyrosine hydroxylase gene promoter. *Brain Res Mol Brain Res*. 2003;112:8-23.

49. Jezova M, Armando I, Bregonzio C, Yu ZX, Qian S, Ferrans VJ, Imboden H, Saavedra JM. Angiotensin II AT(1) and AT(2) receptors contribute to maintain basal adrenomedullary norepinephrine synthesis and tyrosine hydroxylase transcription. *Endocrinology*. 2003;144:2092-2101.

50. Ma FY, Grattan DR, Bobrovskaya L, Dunkley PR, Bunn SJ. Angiotensin II regulates tyrosine hydroxylase activity and mRNA expression in rat mediobasal hypothalamic cultures: the role of specific protein kinases. *J Neurochem*. 2004;90:431-441.

51. Das S, Zhang E, Senapati P, Amaram V, Reddy MA, Stapleton K, Leung A, Lanting L, Wang M, Chen Z et al. A Novel Angiotensin II-Induced Long Noncoding RNA Giver Regulates Oxidative Stress, Inflammation, and Proliferation in Vascular Smooth Muscle Cells. *Circ Res*. 2018;123:1298-1312.

52. Fernandez PM, Brunel F, Jimenez MA, Saez JM, Cereghini S, Zakin MM. Nuclear receptors Nor1 and NGFI-B/Nur77 play similar, albeit distinct, roles in the hypothalamo-pituitary-adrenal axis. *Endocrinology*. 2000;141:2392-400.

53. Kota SK, Meher LK, Jammula S, Mohapatra S, Modi KD. Coexistence of pheochromocytoma with abdominal aortic aneurysm: an untold association. *Ann Med Health Sci Res*. 2013;3:258-261.

54. Arıkan AA. Ruptured abdominal aortic aneurysm with a suprarenal tumor. *Braz J Cardiovasc Surg*. 2018;33:522-524.

Novelty and Significance

What is new?

- This study uncovers the upregulation of the tyrosine hydroxylase (TH) pathway in human and murine AAA, in which TH localizes to vascular innervations, inflammatory cells and scattered VSMC.
- The pharmacological inhibition of TH by AMPT prevents aneurysm development in two experimental models susceptible to AngII-induced AAA.
- In these models, AMPT limits AngII-induced inflammation, MMP activity and ROS production, preserving elastin integrity.

What is relevant?

- Our study evidences that TH upregulation plays a pivotal role on AAA pathophysiology and highlights the potential of pharmacological strategies targeting TH for the treatment of AAA

Summary

The inhibition of TH by AMPT hampers AAA development, limiting vascular remodelling, inflammation and oxidative stress. Our findings support the importance of the induction of

the TH pathway for AAA development and support the interest of novel pharmacological interventions targeting TH for the management of this disease.

Figure Legends

Figure 1. TH is upregulated in human AAA. A) *TH, DBH* and *SLC6A2* mRNA levels were analysed in abdominal aorta from patients with AAA (n= 84) and healthy donors (Do; n= 16). Data, normalised to β-actin expression, are expressed as mean ± SEM. **P*< 0.01, ***P*< 0.0001 *vs*. Donors. **B)** TH protein levels were evaluated by Western blot in these samples. The immunoblot densitometric analysis is shown on left. Data are mean ± SEM (Donors, n= 10; AAA, n= 14). ***P*< 0.0001 *vs*. Donors. **C)** Representative immunohistochemical analysis for TH in human abdominal aortas from donors and patients with AAA. The indicated areas are magnified in middle panels (Bars: 100 μm [upper and lower panels] and 50 μm [middle panels]). TH immunostaining located in vascular nerve endings (GAP43+ cells), lymphocytes (CD3+ cells, red arrowheads), and VSMC (α-SM actin+ cells, black arrowheads). Mann-Whitney (A-C) and t-test (D).

Figure 2. TH is up-regulated in the aneurysmal abdominal aorta from AngII-infused ApoE$^{-/-}$ mice. A) *Th*, *Dbh*, *Ddc* and *Slc6a2* mRNA levels analysed by real-time PCR in abdominal aorta samples from ApoE$^{-/-}$ mice infused with Saline (white bars) or AngII (black bars; 1000 ng/kg/min) for 28 days. Data are expressed as mean ± SEM (Saline-infused ApoE$^{-/-}$ mice, n= 14; AngII-infused ApoE$^{-/-}$ mice, n= 15). **P*< 0.05, ** *P*< 0.01 *vs*. Saline-infused mice. **B)** TH protein levels assessed by Western blot in aortic lysates from these animals. Data are expressed as mean ± SEM (Saline-infused ApoE$^{-/-}$ mice, n= 9; AngII-infused ApoE$^{-/-}$ animals, n= 15). **P*< 0.05 *vs*. Saline-infused ApoE$^{-/-}$ mice. β-actin levels are shown as a loading control. **C)** Representative immunohistochemical analysis for TH in abdominal aortas from saline- and AngII-infused mice. TH immunostaining located in vascular nerve endings (GAP43+ cells), lymphocytes (CD3+ cells, red arrowheads), and VSMC (α-SM actin+ cells,

black arrowheads). The indicated areas are magnified in middle panels (Bars: 100 μm [upper and lower panels] and 50 μm [middle panels]). Mann-Whitney test (A and B).

Figure 3. AMPT prevents AAA in AngII-infused ApoE$^{-/-}$ mice. ApoE$^{-/-}$ mice were infused with Saline or AngII (1000 ng/kg/min) for 28 days. AngII-infused mice were treated or not with α-methyl-*p*-tyrosine (AMPT; 100 mg/Kg twice daily, i.p). **A)** Representative images of excised aortas. **B)** Abdominal aortic diameter was assessed by ultrasonography. Data are mean ± SEM (Saline, n= 9; AngII-infused groups, n= 15). *P*< 0.05: * *vs*. t0 for each experimental condition; # *vs*. Saline-infused mice; $ *vs*. AngII-infused mice non-treated with AMPT. **C)** Transversal and longitudinal ultrasonographic images are shown and the aortic diameter is traced with a yellow line. **D)** Incidence (left) and severity (right; Manning scale)[20] of AAA in AngII-infused ApoE$^{-/-}$ mice treated or not with AMPT. $ *P*< 0.05 *vs*. AngII-infused ApoE$^{-/-}$ mice non-treated with AMPT (n as indicated in B). **E)** Blood pressure levels. Data are mean ± SEM (n as indicated in B). *P*< 0.05: * *vs*. t0 for each experimental condition; # *vs*. Saline-infused mice **F)** Representative haematoxylin-eosin staining of abdominal aortic sections from AngII-infused mice (Bars: 500 μm). Two-way ANOVA with repeated measures (B and E) and chi-square (**D**).

Figure 4. AMPT preserves elastin integrity and ameliorates vascular inflammation and oxidative stress in aorta from AngII-infused ApoE$^{-/-}$ mice. ApoE$^{-/-}$ mice were infused with Saline or AngII (1000 ng/kg/min) for 28 days. AngII-infused mice were treated or not with α-methyl-*p*-tyrosine (AMPT; 100 mg/Kg twice daily, i.p). **A)** Orcein staining of abdominal aortas. Arrowheads mark elastin fibres ruptures. The indicated areas are magnified in lower panels (Bars: 100 μm). Number of elastin fibre ruptures *per* aortic section. Data are mean ± SEM (Saline, n= 5; AngII-infused groups, n= 8). ***P< 0.001 *vs*. Saline-infused animals;

$^{\#}P<0.05$ *vs*. AngII-infused ApoE$^{-/-}$ mice non-treated with AMPT. **B)** MMP activity *per* aortic section assessed by *in situ* zymography (Bars: 50 µm). Data are mean ± SEM (n= 8). $^{*}P<0.05$ *vs*. AngII-infused ApoE$^{-/-}$ mice; $^{\#\#\#}P<0.001$ *vs*. AngII-infused ApoE$^{-/-}$ animals non-treated with AMPT. **C)** mRNA levels of *Mmp2*, *Emr1*, and *Mcp1*, analysed by real-time PCR in abdominal aortas from AngII-treated mice. Data, normalised to *Gapdh* expression, are expressed as mean ± SEM (Saline, n= 9; AngII-infused groups, n= 10). $^{*}P<0.05$, $^{***}P<0.001$ *vs*. Saline-infused mice; $^{\#}P<0.05$, $^{\#\#}P<0.01$, $^{\#\#\#}P<0.001$ *vs*. AngII-infused ApoE$^{-/-}$ mice non-treated with AMPT. **D)** Vascular superoxide anion production visualised by DHE staining (Bars: 50 µm). Data are mean ± SEM (n= 8).$^{*}P<0.05$ *vs*. Saline-infused ApoE$^{-/-}$ mice; $^{\#\#}P<0.01$ *vs*. AngII-infused ApoE$^{-/-}$ mice non-treated with AMPT. One-way ANOVA or Kruskal–Wallis test (A-D).

Figure 5. AMPT prevents aneurysm formation in AngII-infused TgNOR-1^{VSMC} mice. Wild-type (WT) and TgNOR-1^{VSMC} mice were infused with AngII (1000 ng/kg/min) for 28 days). TgNOR-1^{VSMC} mice were treated or not with α-methyl-*p*-tyrosine (AMPT; 100 mg/Kg twice daily, i.p). **A)** Representative images of excised aortas. **B)** Assessment of abdominal aortic diameter by ultrasonography. Data are mean ± SEM (WT mice, n= 10; TgNOR-1^{VSMC} groups, n= 15). $P<0.05$: * *vs*. t0 for each experimental condition; $ *vs*. WT mice; $^{\#}$ *vs*. TgNOR-1^{VSMC} mice non-treated with AMPT. **C)** Representative images of the ultrasonographic analysis. Transversal and longitudinal ultrosonographic images in AngII-challenged mice at 28 days. The aortic diameter is traced with a yellow line. **D)** Incidence (left) and severity (right; Manning scale)[20] of AAA in challenged mice. $P<0.05$: $ *vs*. WT mice; $^{\#}$ *vs*. TgNOR-1^{VSMC} mice non-treated with AMPT (n as indicated in B). **E)** Blood pressure levels. Data are mean ± SEM (WT mice, n= 7; TgNOR-1^{VSMC} groups, n= 12). $^{*}P<0.05$ *vs*. t=0 for each experimental condition. **F)** Representative haematoxylin-eosin staining

of abdominal aortic sections from AngII-infused mice (Bars: 500 µm). Two-way ANOVA with repeated measures (B and E) and chi-square (D).

Figure 6. AMPT limits elastin fibre rupture and ameliorates the increased expression of inflammatory markers and oxidative stress induced by AngII in TgNOR-1^{VSMC} mice. Wild-type (WT) and TgNOR-1^{VSMC} mice were infused with AngII (1000 ng/kg/min) for 28 days. TgNOR-1^{VSMC} mice were treated or not with α-methyl-*p*-tyrosine (AMPT; 100 mg/Kg twice daily, i.p). **A)** Orcein staining of abdominal aortas. Arrowheads mark elastin fibre ruptures. The indicated areas are magnified in lower panels. Bars: 100 µm. The number of elastin fibre ruptures *per* aortic section are shown. Data are mean ± SEM (n= 7). $P< 0.05$: * *vs*. WT mice; $^{\#}$ *vs*. TgNOR-1^{VSMC} mice non-treated with AMPT. **B)** MMP activity *per* aortic section assessed by *in situ* zymography (Bars: 50 µm). Data are mean ± SEM (n= 6). $*P< 0.05$ *vs*. WT mice; $^{\#\#}P< 0.01$ *vs*. TgNOR-1^{VSMC} mice non-treated with AMPT. **C)** mRNA levels of *Mmp2*, *Emr1*, *Mcp1*, *Il6*, *Il1β* and *Cxcl2* in abdominal aortas from each group. Data are expressed as mean ± SEM (WT mice, n=10; TgNOR-1^{VSMC} groups, n= 15). $*P< 0.05$, $**P< 0.01$, $***P< 0.001$ *vs*. WT mice; $^{\#\#}P< 0.01$, $^{\#\#\#}P< 0.001$ *vs*. TgNOR-1^{VSMC} mice non-treated with AMPT. **D)** Vascular superoxide anion production visualised by DHE staining (Bars: 50 µm). Data are represented as mean ± SEM (n= 6). $P< 0.05$: * *vs*. WT mice; $^{\#}$ *vs*. TgNOR-1^{VSMC} mice non-treated with AMPT. One-way ANOVA (C and D) or Kruskal–Wallis test (A and B).

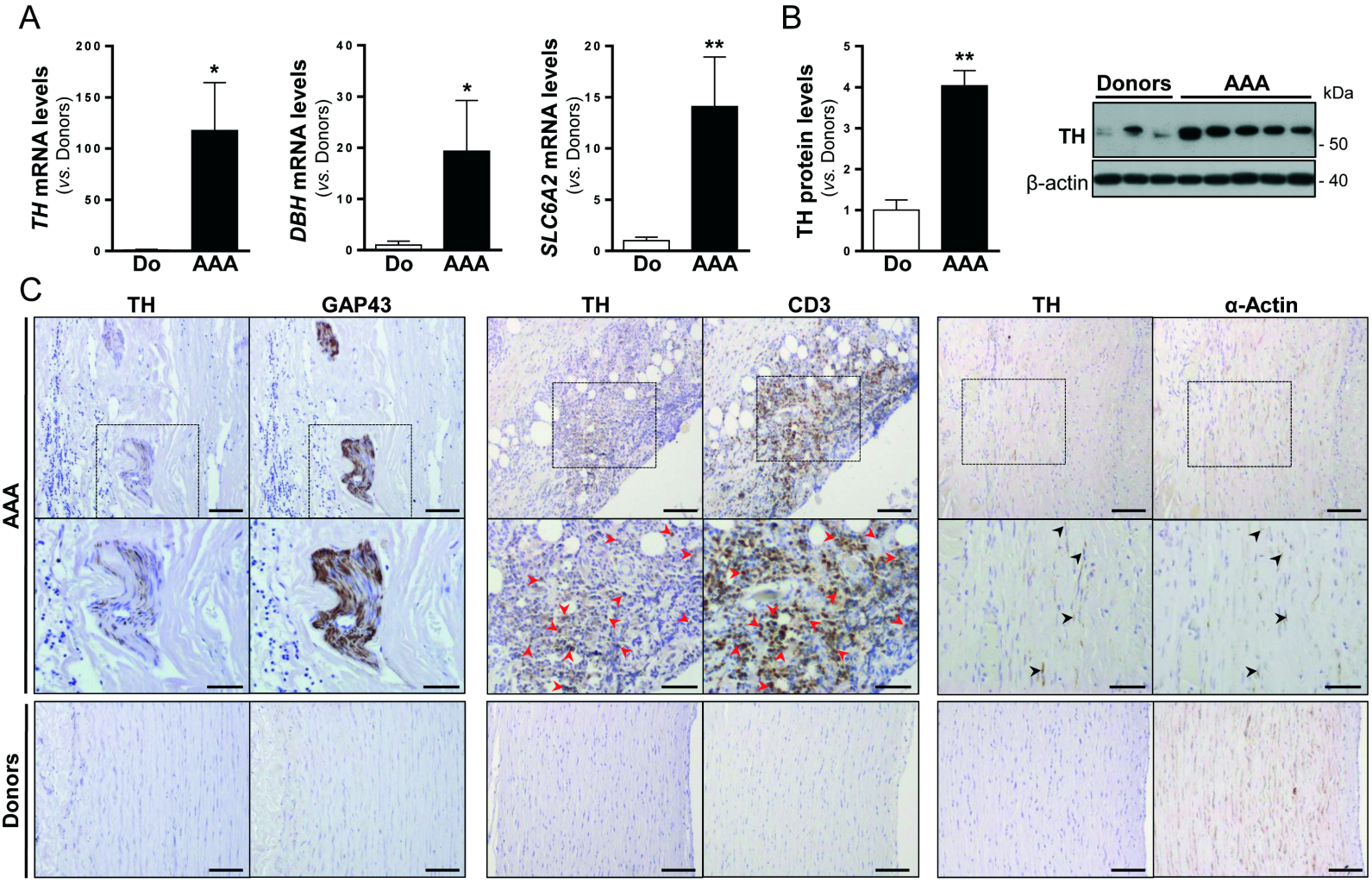
A
TH mRNA levels (vs. Donors)
DBH mRNA levels (vs. Donors)
SLC6A2 mRNA levels (vs. Donors)
Do
AAA
B
TH protein levels (vs. Donors)
Donors
AAA
kDa
TH
β-actin
50
40
C
TH
GAP43
CD3
α-Actin
AAA
Donors

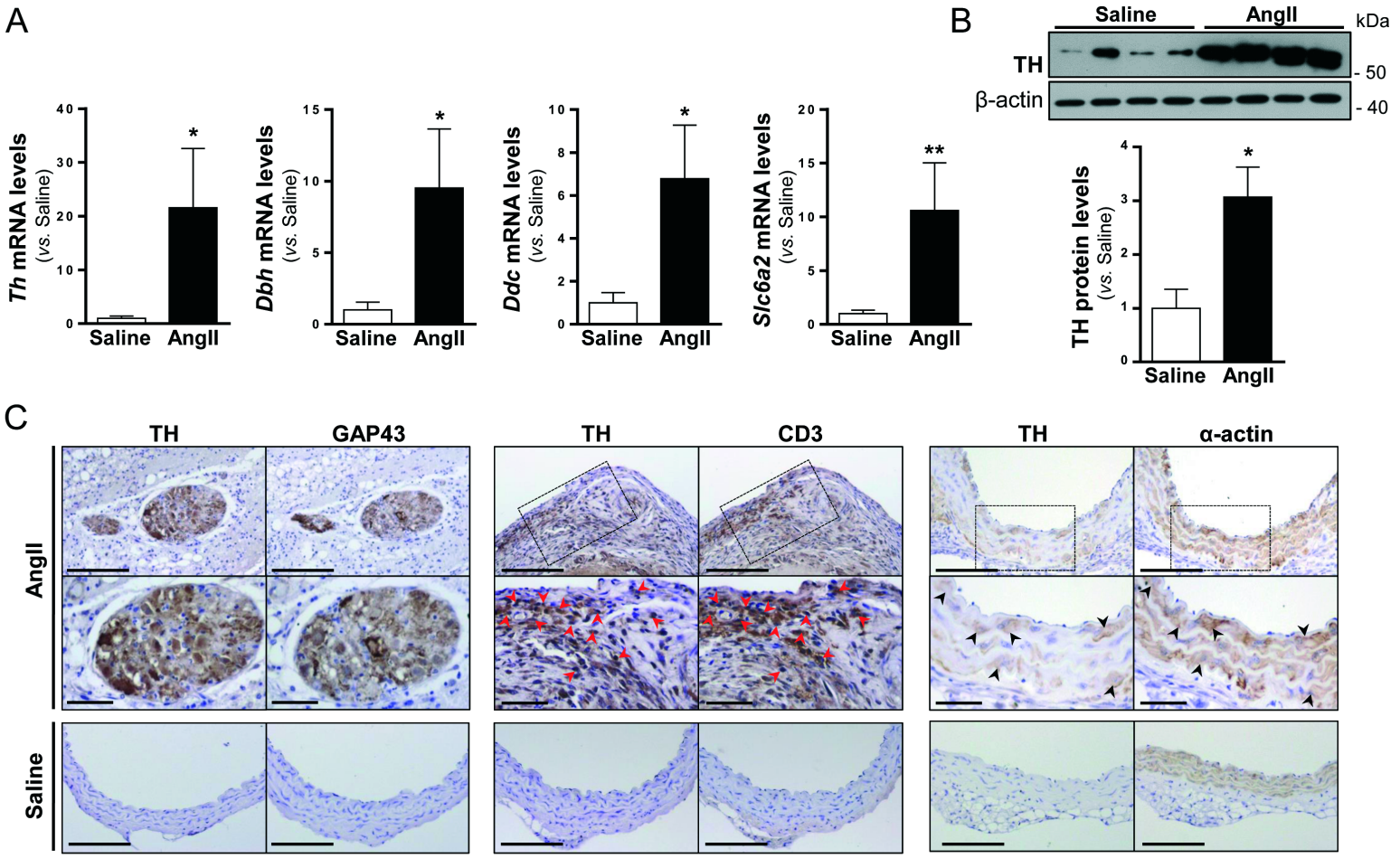
A
Th mRNA levels (vs. Saline)
Dbh mRNA levels (vs. Saline)
Ddc mRNA levels (vs. Saline)
Slc6a2 mRNA levels (vs. Saline)
Saline
AngII
B
Saline
AngII
kDa
TH
β-actin
- 50
- 40
TH protein levels (vs. Saline)
C
TH
GAP43
CD3
α-actin
AngII
Saline

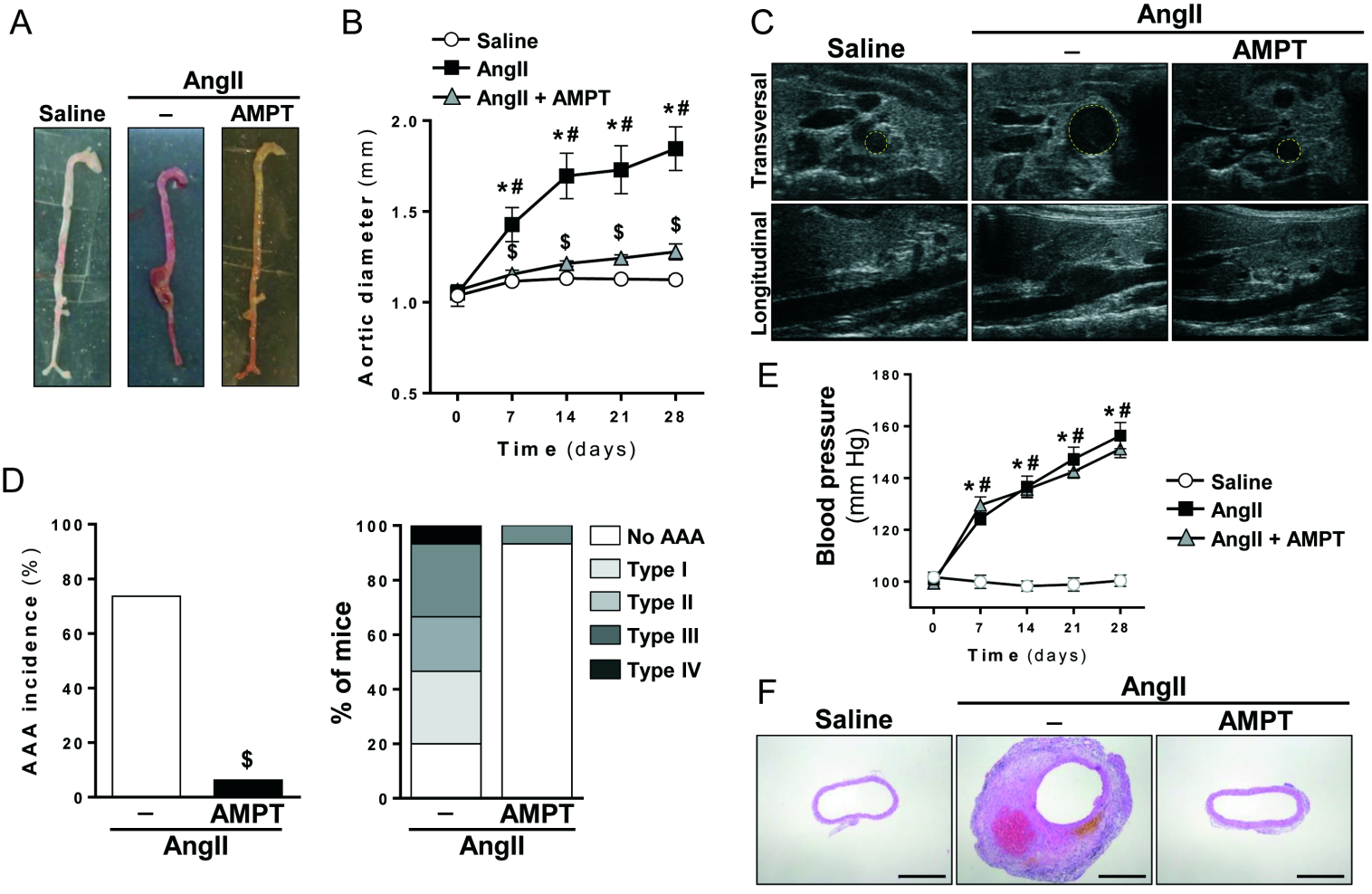
A
Saline
AngII
–
AMPT
B
Saline
AngII
AngII + AMPT
Aortic diameter (mm)
2.0
1.5
1.0
0.5
0
7
14
21
28
Time (days)
*#
$
C
AngII
Saline
–
AMPT
Transversal
Longitudinal
D
AAA incidence (%)
100
80
60
40
20
0
$
–
AMPT
AngII
% of mice
No AAA
Type I
Type II
Type III
Type IV
E
Blood pressure (mm Hg)
180
160
140
120
100
Saline
AngII
AngII + AMPT
F
AngII
Saline
–
AMPT

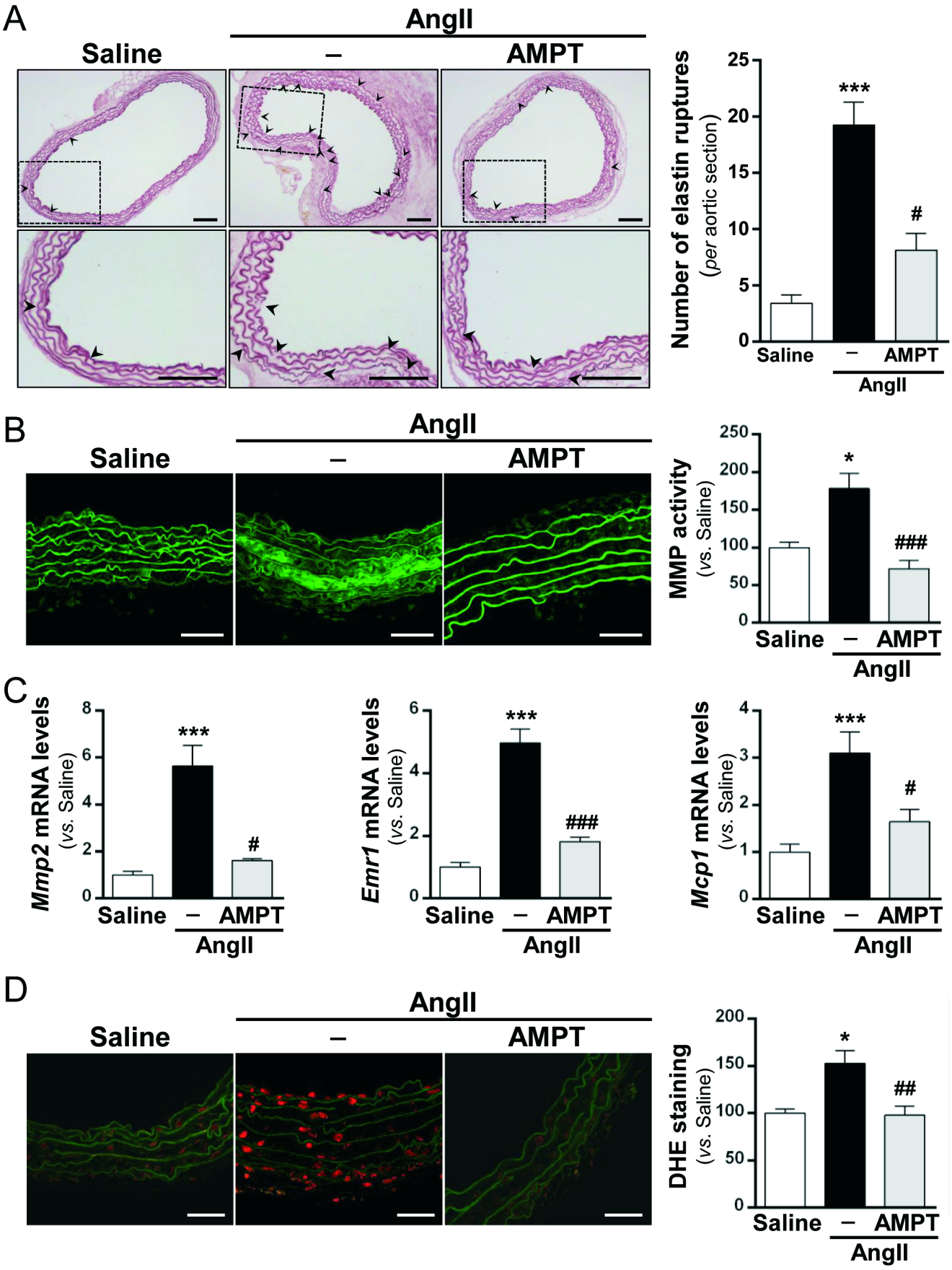
A
AngII
Saline
–
AMPT
Number of elastin ruptures
(per aortic section)
25
20
15
10
5
0
***
#
Saline
–
AMPT
AngII
B
AngII
Saline
–
AMPT
MMP activity
(vs. Saline)
250
200
150
100
50
0
*
###
Saline
–
AMPT
AngII
C
Mmp2 mRNA levels
(vs. Saline)
8
6
4
2
0
***
#
Saline
–
AMPT
AngII
Emr1 mRNA levels
(vs. Saline)
6
4
2
0
***
###
Saline
–
AMPT
AngII
Mcp1 mRNA levels
(vs. Saline)
4
3
2
1
0
***
#
Saline
–
AMPT
AngII
D
AngII
Saline
–
AMPT
DHE staining
(vs. Saline)
200
150
100
50
0
*
##
Saline
–
AMPT
AngII

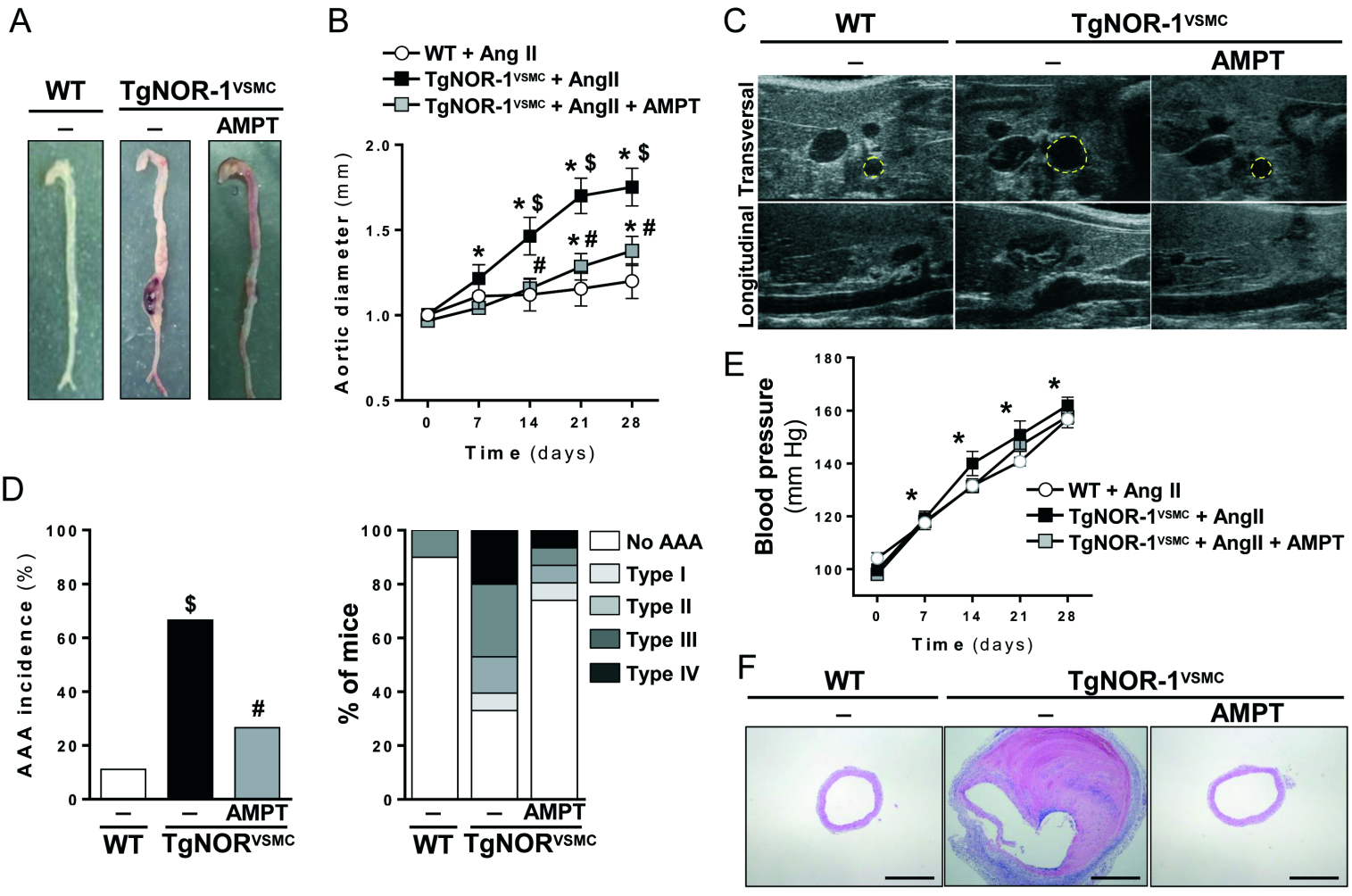
A
WT
TgNOR-1VSMC
–
–
AMPT
B
WT + Ang II
TgNOR-1VSMC + AngII
TgNOR-1VSMC + AngII + AMPT
Aortic diameter (mm)
2.0
1.5
1.0
0.5
0
7
14
21
28
Time (days)
C
WT
TgNOR-1VSMC
–
–
AMPT
Longitudinal
Transversal
D
AAA incidence (%)
100
80
60
40
20
0
$
#
–
–
AMPT
WT
TgNORVSMC
% of mice
No AAA
Type I
Type II
Type III
Type IV
E
Blood pressure (mm Hg)
180
160
140
120
100
WT + Ang II
TgNOR-1VSMC + AngII
TgNOR-1VSMC + AngII + AMPT
Time (days)
F
WT
TgNOR-1VSMC
–
–
AMPT

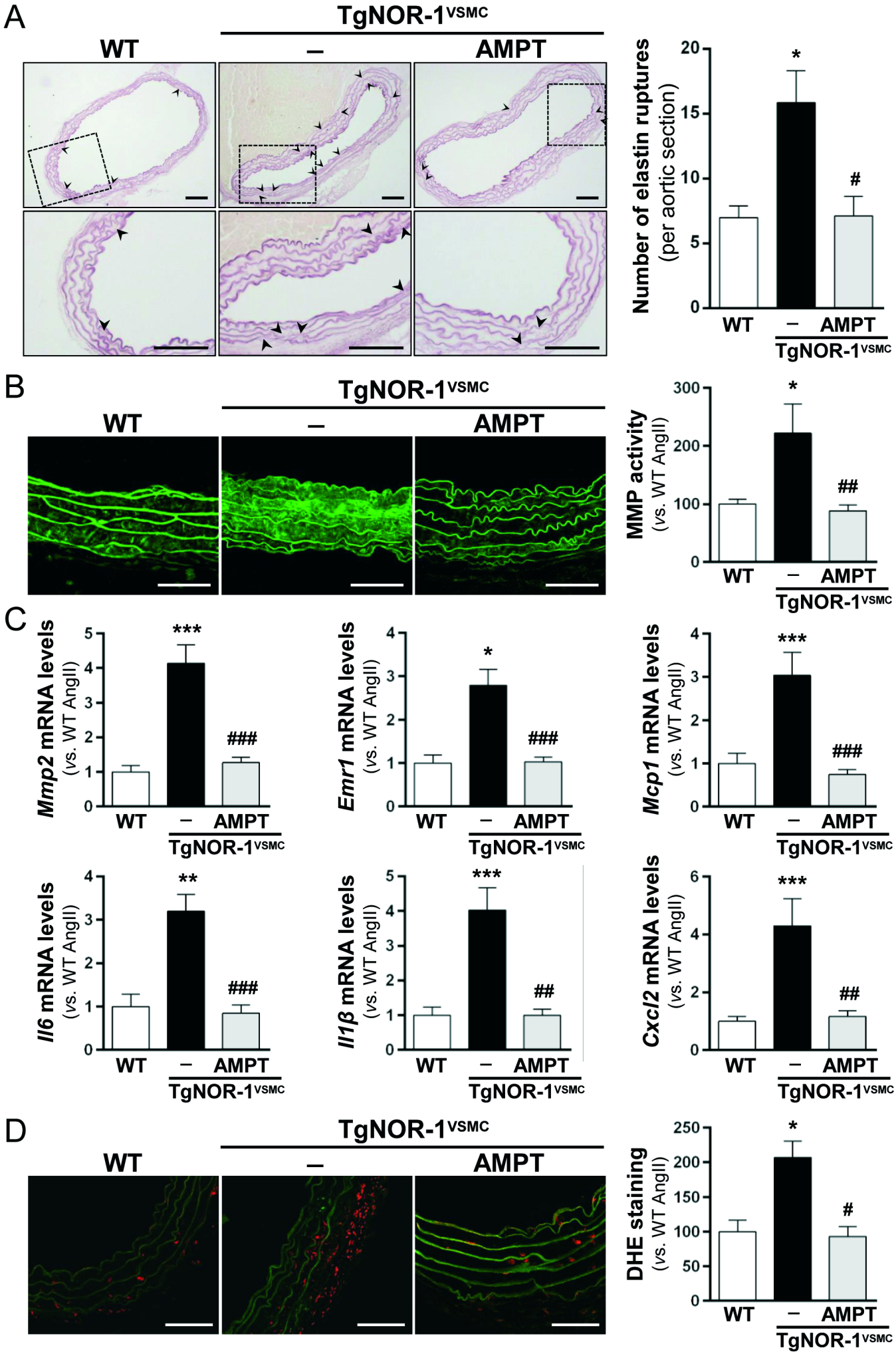
A
TgNOR-1VSMC
WT
–
AMPT
Number of elastin ruptures
(per aortic section)
20
15
10
5
0
*
#
WT
–
AMPT
TgNOR-1VSMC
B
TgNOR-1VSMC
WT
–
AMPT
MMP activity
(vs. WT AngII)
300
200
100
0
*
##
WT
–
AMPT
TgNOR-1VSMC
C
Mmp2 mRNA levels
(vs. WT AngII)
***
###
Emr1 mRNA levels
(vs. WT AngII)
*
###
Mcp1 mRNA levels
(vs. WT AngII)
***
###
Il6 mRNA levels
(vs. WT AngII)
**
###
Il1β mRNA levels
(vs. WT AngII)
***
##
Cxcl2 mRNA levels
(vs. WT AngII)
***
##
WT
–
AMPT
TgNOR-1VSMC
D
TgNOR-1VSMC
WT
–
AMPT
DHE staining
(vs. WT AngII)
250
200
150
100
50
0
*
#
WT
–
AMPT
TgNOR-1VSMC

Supplemental Material

Targeting tyrosine hydroxylase for abdominal aortic aneurysm: impact on inflammation, oxidative stress and vascular remodeling

Laia Cañes[1,2,3], Judith Alonso[1,2,3], Carme Ballester-Servera[1,3], Saray Varona[1,2,3], José R Escudero[2,4], Vicente Andrés[2,6], Cristina Rodríguez[2,3,5*] and José Martínez-González[1,2,3,*]

[1]Instituto de Investigaciones Biomédicas de Barcelona (IIBB-CSIC), Barcelona, Spain.
[2]CIBER de Enfermedades Cardiovasculares, ISCIII, Madrid, Spain.
[3]Instituto de Investigación Biomédica Sant Pau, Barcelona, Spain.
[4]Servicios Mancomunados de Angiología, Cirugía Vascular y Endovascular, Hospitales de la Santa Creu i Sant Pau/Dos de Mayo, Barcelona, Spain.
[5]Institut de Recerca Hospital de la Santa Creu i Sant Pau (IRHSCSP), Barcelona, Spain.
[6]Centro Nacional de Investigaciones Cardiovasculares (CNIC), Madrid, Spain.

Short title:TH in abdominal aortic aneurysm.

[*]These authors contributed equally to this work. Correspondence should be addressed to J.M.-G. IIBB, Rosselló, 161, 08036 Barcelona, Spain (email: jose.martinez@iibb.csic.es; pone: +34935565896) or C.R. IRHSCSP, C/Antoni Mª Claret, 08025 Barcelona, Spain (email: crodriguezs@santpau.cat; phone: +34935565897).

MATERIAL AND METHODS

Aneurysm and donor sampling and preservation

Human abdominal aortic samples were obtained from patients subjected to open repair surgery for AAA at the Hospital de la Santa Creu i Sant Pau (HSCSP; Barcelona, Spain), while healthy specimens come from multi-organ donors, as previously described.[1,2] The study was approved by the HSCSP Ethics Committee (IIBSP-NET-2019-40) and conducted according to the Declaration of Helsinki. An informed consent from patients and control individuals or from their legal representatives was obtained. Control samples were examined to exclude the presence of aneurysmal or atherosclerotic lesions or other abnormalities that could affect the study. Samples were immediately stored at −80 °C for subsequent RNA or protein extraction or processed for immunohistochemical analysis.

Animal handling

Two animal models were used: apolipoprotein E-deficient ($ApoE^{-/-}$) mice (Charles River Ltd; Kent, UK) and a mouse model that specifically over-expresses the human nuclear receptor NOR-1 in the vascular wall ($TgNOR\text{-}1^{VSMC}$).[3,4] Transgenic mice and their control littermates (wild-type; WT) on C57BL/6J genetic background were bred in the Animal Experimentation Unit (Institut de Recerca de l'Hospital de la Santa Creu i Sant Pau [IRHSCSP], Barcelona, Spain). All the procedures followed the principles and guidelines established by the Spanish Policy for Animal Protection RD53/2013 and the European Union Directive 2010/63/UE and were approved by the IRHSCSP ethical committee (Law 5/June 21, 1995; Generalitat de Catalunya).

Due to the sexual dimorphism characterizing AAA, with higher prevalence in males both in humans and animal models, the studies were exclusively performed in male mice. Three-month-old male mice were infused with angiotensin II (AngII [1000 ng/kg body weight (BW)/min; Sigma-Aldrich, St Louis, MO, USA]) for 28 days via osmotic minipumps (model 1004, Alzet; Durect Corporation, Cupertino, CA, USA).[5] Mice were anaesthetised by isofluorane inhalation (1.5%) and osmotic minipumps were subcutaneously implanted in the scapular region. After surgery, animals were kept warm on a heating pad until awake and closely supervised. AngII-infused mice were pre-treated or not with doxycycline (Sigma-Aldrich; 30 mg/kg/day in the drinking water)[6] or with a tyrosine hydroxylase inhibitor (α-methyl-*p*-tyrosine [AMPT; Sigma-Aldrich]) throughout the 28 days experimental period. AMPT was administered twice daily (100 mg/Kg, i.p), early in the morning (9 p.m.) and late in the afternoon (18:00 pm).[7] All treatments started 24 h before AngII infusion. Analysis were also performed in a early stage of AAA pathogenesis. For this purpose, three-month-old male $ApoE^{-/-}$ mice were infused with AngII (1000 ng/kg BW/min; Sigma-Aldrich, St Louis, MO, USA]) for 5 days via osmotic minipumps (model 1007D, Alzet). Three-month-old male WT, $ApoE^{-/-}$ and transgenic mice were used as controls. Sample size was calculated on the basis of previous studies.[5] Animals were randomly distributed among groups by an operator unaware of the nature of the experiments.

Non-invasive measurement of systolic blood pressure

Blood pressure measurements were non-invasively performed in conscious mice prior to and following treatments by the tail-cuff plethysmography method (CODA® tail-cuff blood pressure system; Kent Scientific Corporation; Torrington, CT, USA). To get reliable pressure measurements, mice were habituated to the tail-cuff procedure over

five consecutive days before the implantation of minipumps. To avoid the influence of the circadian cycle blood pressure measurements were always performed at the same time (between 9 a.m. and 11 a.m.).[5,6]

Measurement of abdominal aortic diameter by ultrasonography

Mice were anaesthetised with 1.5% isofluorane inhalation as indicated above and lightly secured in the supine position to a warming platform. The abdominal region was shaved and an echography was performed to determine abdominal aorta diameter using a Vevo 2100 ultrasound with a 30 MHz transducer (VisualSonics, Toronto, ON, Canada).[5,6] Abdominal aortas with diameters ≥1.5 mm were considered as aneurysms. All primary measurements were made from images captured on cine loops of 100 frames at the time of the study using the software provided by the echography machine.

Ultrasonographic data was registered at baseline and weekly throughout the experimental period. Once the experimental procedure was completed, mice were euthanised via isofluorane overdose. The severity of the aneurysm was established on the basis of a 0 to 4-point grading scale previously detailed:[8] type 0, lack of aneurysm; type I, dilated lumen of the suprarenal aorta without thrombus; type II, vascular remodelling of suprarenal aorta that frequently contained thrombus; type III, a pronounced bulbous aneurysmal form of type II that contained thrombus, and type IV, characterized by the presence of multiple AAAs containing thrombus. All measurements were performed by an experienced and blinded operator.

Lipid profile and markers of hepatic and renal function in plasma

Triglycerides and total cholesterol levels were quantified with a colorimetric assay in plasma from ApoE$^{-/-}$ mice by using specific reagents (Gernon, GN90125 and GN20125, respectively; RAL Técnica para el Laboratorio S.A., Barcelona, Spain) and a multicuvette rack reader (Clima MC-15, RAL Técnica para el Laboratorio S.A.) following manufacturers' recommendations. Plasma levels of aspartate transaminase (AST), alanine transaminase (ALT), creatinine and blood urea nitrogen (BUN) were quantified using a Cobas 6000/c501 autoanalyser and specific reagents (Roche Diagnostics International Ltd, Basel, Switzerland).[5]

Enzyme-linked immunosorbent assay (ELISA)

Noradrenaline (NA) concentrations in plasma were determined using the Noradrenaline High Sensitive ELISA kit (ref: EA633/96; DLD Diagnostika GmbH, Hamburg, Germany). Blood samples were drawn between 11:00 and 12:00 a.m. EDTA anticoagulated plasma was obtained by centrifugation at 1200 x*g* 10 min at 4 ºC. The sample stabilizer of the kit was added to each sample and plasma was immediately frozen. Samples were analyzed at most one week after collection.

Analysis of mRNA levels

Total RNA was isolated using TRIsure™ reagent (Bioline) and reverse transcribed into cDNA using the High Capacity cDNA Reverse Transcription Kit (Applied Biosystems). Quantification of mRNA levels was performed by real-time PCR using the ABI PRISM 7900HT sequence detection system (Applied Biosystems). Specific primers and probes (provided by Applied Biosystems or Integrated DNA Technologies Inc, Coralville, IA, USA.) were used for the quantification of human mRNA levels for *TH* (HS.PT.58.369742), dopamine β-hydroxylase (*DBH*; Hs.PT.58.39251730), solute carrier family 6 member 2 (*SLC6A2*, Hs.PT.58.45584874), and β-actin (*ACTB*, Hs99999903_m1; used as reference gene). To assess mRNA levels in mouse tissues the

following primers and probes were used for *Th* (Mm.PT.58.33106180), interleukin-6 (*Il6*; Mm00446191_m1), *Il1β* (Mm00434228_m1), C-C motif chemokine ligand 2 (*Ccl2 or Mcp1* (Mm00441242_m1), metalloproteinase-2 (*Mmp2;* MmPT.58.9606100), EGF-like module-containing mucin-like hormone receptor-like 1 (*Emr1*;MmPT.56a.11087779), C-X-C Motif Chemokine Ligand 2 (*Cxcl2*; Mm00436450_m1), tenascin C (*Tnc*; Mm00495662_m1), and neutrophil gelatinase-associated lipocalin (*Ngal*; Mm01324470_m1). Further, specific primers for SYBR Green real-time PCR analysis were used for the assessment of *Slc6a2* (5'-CTGGCTCTGGGGCAATACAAG-3' and 5'- GCCGACATAGAGGGCAATGA-3'), *Dbh* (5'-CGAGGAGAGATGGAGAACGC-3' and 5'-ATCTCGAGTCCTCTGTGCCT-3') and dopa decarboxylase (*Ddc*, 5'-GCCTTTTTGGCTGGAAGAGC-3' and 5'-GCTTGTGTGAACTCTGGGGA-3'). Glyceraldehyde-3-phosphate dehydrogenase (*Gadph*; Mm.PT.58.39a.1) expression was used as a reference gene for mouse tissues.

In situ detection of vascular $O_2^{\cdot-}$ production

The *in situ* production of $O_2^{\cdot-}$ was assessed using the fluorescent dye dihydroethidium (DHE, Sigma-Aldrich Co.). For this purpose, arterial segments were soaked in PBS with 30% sucrose for 20–50 min, embedded in Tissue Tek OCT embedding medium (Sakura Finetek Europe B.V., Alphen aan den Rijn, The Netherlands), and frozen in liquid nitrogen. DHE (2 μM) was applied onto each section previously equilibrated for 30 min at 37 °C in Krebs-HEPES buffer (in mM: 130 NaCl, 5.6 KCl, 2 $CaCl_2$, 0.24 $MgCl_2$, 8.3 HEPES, 11 glucose, pH = 7.4). Then sections were cover-slipped and incubated for 30 min in a light-protected humidified chamber at 37 °C. Fluorescence was visualised with a fluorescent laser scanning confocal microscope (Leica TCS SP2 equipped with a krypton/argon laser, 40x objective; Leica Microsistemas S.L.U.). Fluorescence was detected with a 568 nm long-pass filter establishing the same image settings for all experimental conditions. To minimize laser fluctuations from one day to another, data were expressed as % of signal in control arteries.[9]

Immunoblotting

Protein homogenates were separated on SDS-polyacrylamide gels and transferred to polyvinylidene diflouride membranes (Immobilon, Merck-Millipore; IPVH00010). Blots were incubated with antibodies directed against TH (ab75875, Abcam, Cambridge, UK) and β-actin (A5441, Sigma-Aldrich). After incubation with appropriate HRP-conjugated secondary antibodies (Dako Products, Agilent, Santa Clara, CA, USA) blots were incubated with SuperSignal West Dura Extended Duration Substrate (Thermo Fisher Scientific). Protein molecular-mass standards (Hyperpage Prestained Protein Marker; Bioline, Paris, France) allowed to evaluate the size of detected proteins. Ponceau staining and β-actin levels confirmed equal loading and transfer of protein.

Histological, immunohistochemical and immunocytochemical analysis

Aortas were fixed in 4% paraformaldehyde/0.1 M PBS (pH 7.4) for 24 hours, embedded in paraffin and sectioned (5 μm). Then, sections were deparaffinised in xylene, rehydrated in graded series of ethanol and rinsed in distilled water. Endogenous peroxidase activity was blocked using a 3% hydrogen peroxide solution in methanol for 30 min. Afterwards, sections were blocked with 10% normal serum and incubated with antibodies against MAC3 (sc-19991, Santa Cruz Biotechnology), CD3 (A0452, Dako, Agilent Technologies Co., Hamburg, Germany), α-SM actin (ab5694, Abcam), MCP1

(sc-1785, Santa Cruz Biotechnology Inc.), elastase, neutrophil expressed (ELANE; M0752, Dako, Agilent Technologies Co., Hamburg, Germany), Growth Associated Protein 43 (GAP43; ab75810, Abcam) or MMP2 (ab51125, Abcam). After washing, slides were exposed for 1 h to a biotinylated secondary antibody (Vector Laboratories, Burlingame, CA, USA). After extensive washing with PBS, the Vectastain (ABC) avidin-biotin peroxidase complex (Vector Laboratories) was applied, and the slides were incubated for 30 min. Colour development was achieved with 3,3'-diaminobenzidine (DAB). Then, slides were counterstained with haematoxylin, dehydrated, cleared, and mounted. Negative controls where the primary antibody was omitted allowed to exclude non-specific binding. The histological characterization of aortic samples was performed by haematoxylin-eosin staining. A blinded operator carried out the quantitative morphological assessment of luminal and outer abdominal aortic areas performed by image analysis on haematoxylin-eosin stained sections using ImageJ software. Aortic samples were also subjected to orcein staining (Casa Álvarez, Madrid, Spain) for the analysis of elastic fibre integrity.

In situ Zymography

Gelatinolytic activity was assessed using the Quenched Fluorogenic DQ^{TM} gelatine (D-12054, Thermo Fisher Scientific) as a fluorogenic substrate, as we previously reported.[5] Briefly, DQ-gelatine was dissolved in water at 1 mg/mL and then diluted 1:10 in 1% (w/v) low gelling temperature agarose (A9414, Sigma). The mixture was applied onto OCT-embedded unfixed frozen tissue sections (8 µm) and cover-slipped. After gelatine gelling by incubation at 4 ºC for 30 min, samples were kept at room temperature for 24 h in darkness. FITC fluorescence was visualised with a Leica TCS SP5 confocal microscopy (excitation wavelength: 495 nm; emission wavelength: 515 nm) and the Leica LAS AF Lite software. Samples pre-incubated with 20 mM EDTA before the addition of the labelled substrate were used as negative controls.

Vascular smooth muscle cells (VSMC) culture

Mouse and rat aortic VSMC were obtained by the explants technique as previously described.[3] Briefly, endothelium denuded medial tissue was cut into 1-2 mm cubes that were transferred to a 25 cm^2 culture flask containing 5 ml of pre-warmed DMEM supplemented with 10% foetal calf serum (FCS; Biological Industries, Kibbutz Beit-Haemek, Israel) and antibiotics (100 U/ml penicillin and 0.1 mg/ml streptomycin). VSMC migrate out from the explants within 2-3 weeks. Cells were used between passages 3 to 5. Rat VSMC were seeded in multiwell plates to be used in transfection experiments. Mouse VSMC were maintained in standard culture conditions until subconfluence. Then cells were treated or not with Ang II (10^{-7} M; 1, 2, or 6 h) and RNA was isolated as described above.

Generation of *TH* promoter constructs and luciferase reporter assays

The human *TH* promoter (positions -3639 to -163 relative to the Transcription Start Site [TSS]; ENSG00000180176) was amplified by PCR from genomic DNA. The primers used were: 5´- TATACTCGAGCCCCTGGTCACCTGTTTTGT -3' (forward; *Xho*I site is underlined) and 5'- TATAAGATCTGGCTCGTCCGTGGAATCTAA -3' (reverse; *Bgl*II site is underlined). The PCR product was cloned into the pGL3 vector (Promega, Madison, WI, USA) (pGL3/pTH–3639). A putative NBRE (-2350/-2344) site located in *TH* promoter was mutated using the QuikChange^{TM} Site-Directed Mutagenesis Kit (Agilent Technologies, Santa Clara, CA, USA) and primers (Table S3). These constructs were used in transient transfection assays in rat VSMC as previously

described.[24] Transfections were performed in 12-well plates using 0.5 µg of the luciferase reporter plasmid together with the pCMV5/NOR-1 expression vector or the pCMV5 empty vector (0.05 µg), 0.5 µl PLUS™ Reagent and 1.25 µl of Lipofectamine™ LTX Reagent (ThermoFisher Scientific, Waltham, MA, USA) per well. The pRL-SV40 (25 ng) was included as an internal control (Promega). Firefly and renilla luciferase activities were measured with the Dual-Luciferase™ Reporter Assay System (Promega) in a luminometer (Orion I; Berthold Detection Systems, Pforzheim, Germany). Results were expressed as the ratio of Firefly to Renilla activity.

REFERENCES

1. Orriols M, Varona S, Martí-Pàmies I, Galán M, Guadall A, Escudero JR, Martín-Ventura JL, Camacho M, Vila L, Martínez-González J, et al. Down-regulation of Fibulin-5 is associated with aortic dilation: role of inflammation and epigenetics. *Cardiovasc Res*. 2016;110:431-442.
2. Alonso J, Galán M, Martí-Pàmies I, Romero JM, Camacho M, Rodríguez C, Martínez-González J. NOR-1/NR4A3 regulates the cellular inhibitor of apoptosis 2 (cIAP2) in vascular cells: role in the survival response to hypoxic stress. *Sci Rep*. 2016;6:34056.
3. Rodríguez-Calvo R, Guadall A, Calvayrac O, Navarro MA, Alonso J, Ferrán B, de Diego A, Muniesa P, Osada J, Rodríguez C et al. Over-expression of neuron-derived orphan receptor-1 (NOR-1) exacerbates neointimal hyperplasia after vascular injury. *Hum Mol Genet*. 2013;22:1949-1959.
4. Cañes L, Martí-Pàmies I, Ballester-Servera C, Herraiz-Martínez A, Alonso J, Galán M, Nistal JF, Muniesa P, Osada J, Hove-Madsen L, et al. Neuron-derived orphan receptor-1 modulates cardiac gene expression and exacerbates angiotensin II-induced cardiac hypertrophy. *Clin Sci (Lond)*. 2020;134:359-377.
5. Cañes L, Martí-Pàmies I, Ballester-Servera C, Alonso J, Serrano E, Briones AM, Rodríguez C, Martínez-González J. High neuron derived orphan receptor-1 (NOR-1) expression strengthens the vascular wall response to angiotensin II leading to aneurysm formation in mice. *Hypertension*. 2021;77:557-570.
6. Galán M, Varona S, Orriols M, Rodríguez JA, Aguiló S, Dilmé J, Camacho M, Martínez-González J, Rodriguez C. Induction of histone deacetylases (HDACs) in human abdominal aortic aneurysm: therapeutic potential of HDAC inhibitors. *Dis Model Mech*. 2016;9:541-552.
7. Meltzer HY, Fessler RG, Simonovic M, Doherty J, Fang VS. Effect of d- and l-amphetamine on rat plasma prolactin levels. *Psychopharmacology (Berl)*. 1979;61:63-69.
8. Manning MW, Cassis LA, Daugherty A. Differential effects of doxycycline, a broad-spectrum matrix metalloproteinase inhibitor, on angiotensin II-induced atherosclerosis and abdominal aortic aneurysms. *Arterioscler Thromb Vasc Biol*. 2003;23:483-488.
9. Martínez-Revelles S, García-Redondo AB, Avendaño MS, Varona S, Palao T, Orriols M, Roque FR, Fortuño A, Touyz RM, Martínez-González J, et al. Lysyl oxidase induces vascular oxidative stress and contributes to arterial stiffness and abnormal elastin structure in hypertension: role of p38MAPK. *Antioxid Redox Signal*. 2017;27:379-397.

Table S1. Patients and donors clinical features

Clinical parameters	Donors (*n* = 16)	AAA (*n* = 86)
Age (years ± SD)	63.5 ± 15.7	71.3 ± 6.1
Males (%)	81	100
Smoking (%)*	43.8	79.1
Hypertension (%)	50	69.8
Diabetes (%)	37.5	11.6
Hyperlipidemia (%)	18.8	65.1
Ischemic cardiomyopathy(%)	0	16.3

* Current and ex-smokers. AAA, abdominal aortic aneurysm; SD, standard deviation.

Table S2. Patients and donors clinical features included in Figure 1B

Clinical parameters	Donors (*n* = 10)	AAA (*n* = 14)
Age (years ± SEM)	65.9 ± 3.3	79 ± 1.8
Males (%)	80	100
Smoking (%)*	50	79
Hypertension (%)	50	64
Diabetes (%)	30	14
Hyperlipidemia (%)	20	64
Ischemic cardiomyopathy(%)	0	14

* Current and ex-smokers. AAA, abdominal aortic aneurysm; SEM, standard error of the mean.

Table S3. Body weight and plasma lipids in ApoE$^{-/-}$ mice.

	ApoE$^{-/-}$/Saline	ApoE$^{-/-}$/AngII	ApoE$^{-/-}$ / AngII/ AMPT
BW (g)	28.0 ± 1.85	27.9 ± 1.6	29.5 ± 2.6
Total Chol (mg/dL)	466.8 ± 36.7	464.4 ± 35.8	492.2 ± 10.3
TG (mg/dL)	127.7 ± 39.8	158.5 ± 40.1	137.4 ± 34.01
n	9	10	11

BW: body weight; Chol: cholesterol; TG: triglycerides.

Table S4. Oligonucleotides used for mutagenesis studies

Forward primer	5'-CACTGCCGGATGTGGATTTaaCAATTCAGCAAATGTCTTCCAC-3'
Reverse primer	5'-GTGGAAGACATTTGCTGAAttGTTAAATCCACATCCGGCAGTG-3'

NBRE site (at -2350 bp) is underlined and changes are indicated in lower case letters.

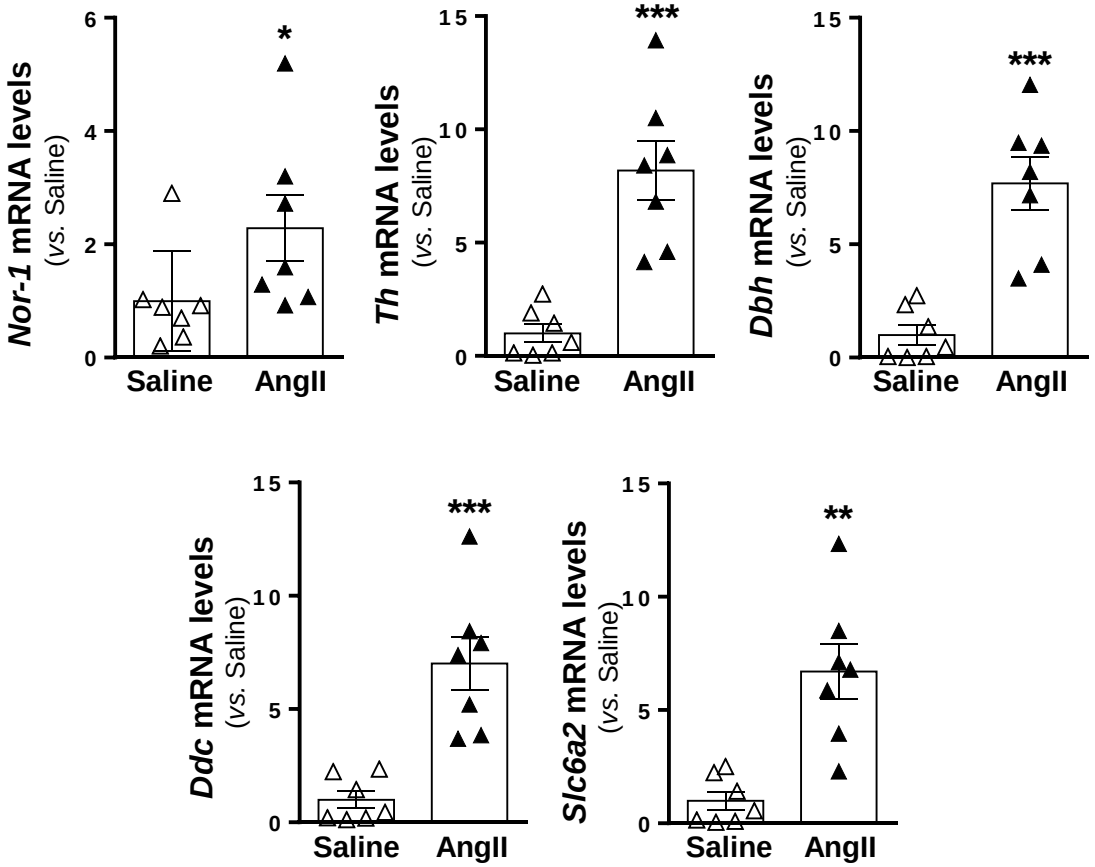

Figure S1. NOR-1 and the TH pathway are upregulated in the early stages of experimental AAA. *Nor-1, Th, Dbh* and *Slc6a2* mRNA levels were analysed in abdominal aortas from ApoE$^{-/-}$ mice infused with saline (open symbols) or AngII (filled symbols; 1000 ng/kg/min) for 5 days (n= 7). Data, normalised to β-actin expression, are expressed as mean ± SEM. **P*< 0.05, ***P*< 0.01, ****P*< 0.001 *vs*. saline-infused mice. Mann-Whitney test.

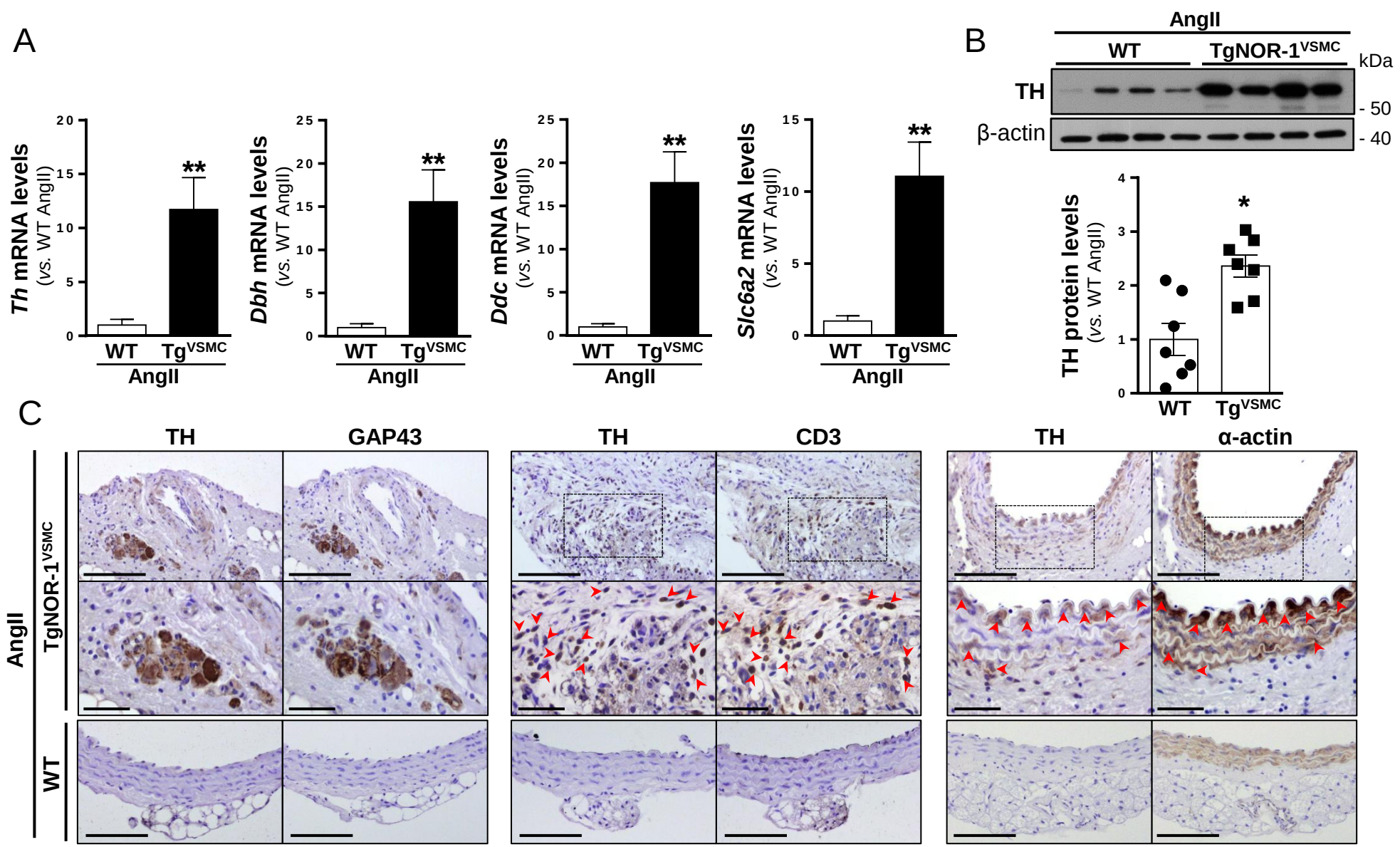

Figure S2. TH is up-regulated in the aneurysmal abdominal aorta from AngII-infused TgNOR-1^{VSMC} mice. A) *Th*, *Dbh*, *Ddc* and *Slc6a2* mRNA levels analysed by real-time PCR in abdominal aorta samples from Wild-type (WT; white bars) and TgNOR-1^{VSMC} (Tg^{VSMC}; black bars) mice infused with AngII (1000 ng/kg/min) for 28 days. Data are mean ± SEM (WT mice, n= 10; TgNOR-1^{VSMC} mice, n= 15). ***P*< 0.001 *vs*. WT mice. **B)** Aortic TH protein levels assessed by Western blot in AngII-infused WT (circles) or Tg^{VSMC} (squares) mice. Data are expressed as mean ± SEM (AngII-infused WT and TgNOR-1^{VSMC}mice, n= 7). **P*< 0.01 *vs*. AngII-infused WT mice. **C)** Representative immunohistochemical analysis for TH in abdominal aortas. TH immunostaining located in vascular nerve endings (GAP23+ cells), lymphocytes (CD3+ cells, red arrowheads), and VSMC (α-SM actin+ cells, red arrowheads). The indicated areas are magnified in right panels (Bars: 100 µm [upper and lower panels] and 50 µm [lmiddle panels]). Mann-Whitney test (A and B).

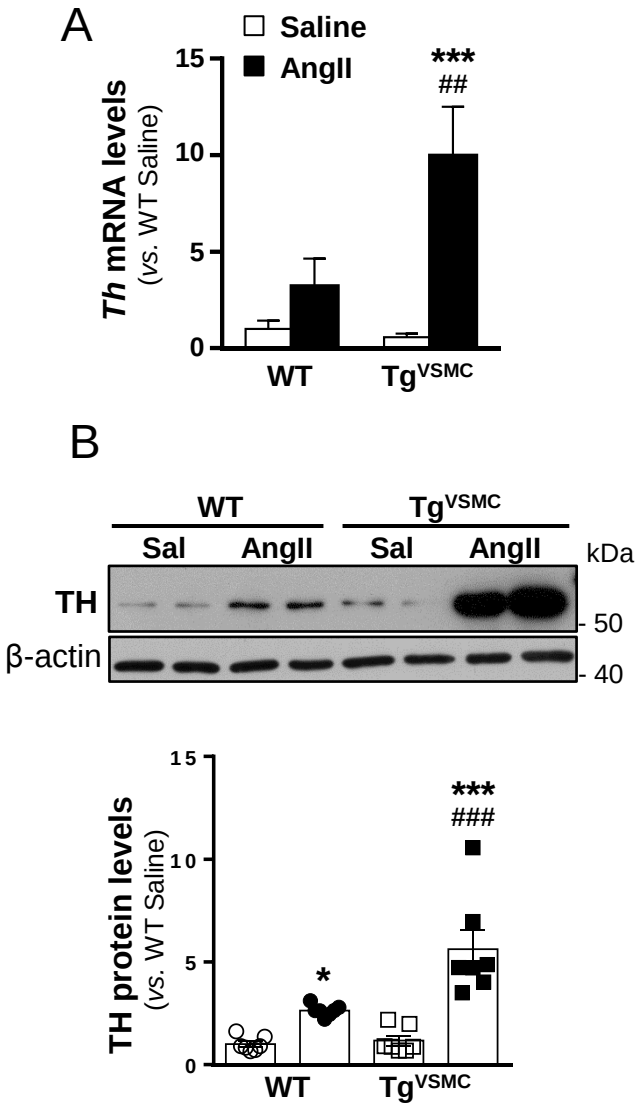

Figure S3. **Angiotensin II (AngII) increases aortic TH expression in TgNOR-1^{VSMC} mice. A)** *Th* mRNA levels were assessed by real-time PCR in abdominal aorta samples from WT and TgNOR-1^{VSMC} (Tg^{VSMC}) mice infused with saline (Sal; white bars) or AngII (1000 ng/kg/min for 28 days; black bars). Data normalised to GAPDH expression represent mean ± SEM (n= 15). **B)** TH protein levels were assessed in these samples by Western-blot (Sal; open symbols and AngII; filled symbols). Levels of β-actin are shown as a loading control. Protein size was estimated by the indicated position of molecular weight markers. The immunoblot densitometric analysis is shown in the lower panel. Data are mean ± SEM (n= 7). *P< 0.05, ***P< 0.001 *vs*. saline-infused mice; $^{\#\#}P$< 0.01, $^{\#\#\#}P$< 0.001 *vs*. AngII-infused WT mice. Two-way ANOVA (A-B).

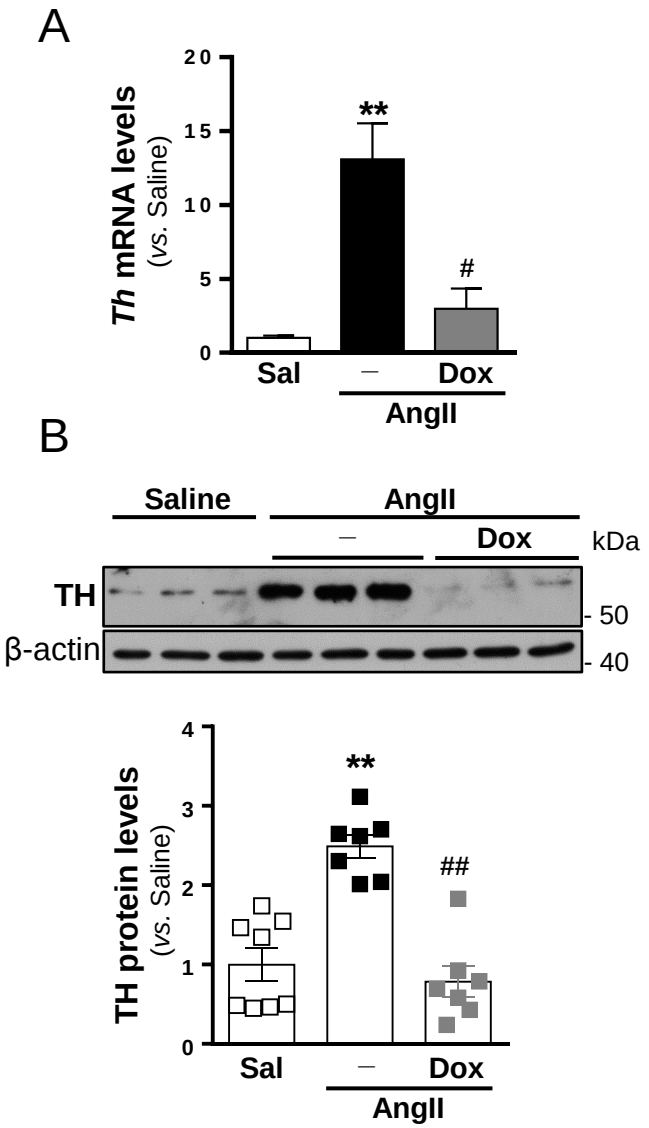

Figure S4. **Doxycycline prevents the increase in aortic TH expression induced by AngII-infusion in TgNOR-1^{VSMC} mice. A)** *Th* mRNA levels analysed by real-time PCR in abdominal aorta samples from TgNOR-1^{VSMC} mice infused with saline (Sal) or AngII (1000 ng/kg/min for 28 days) treated or not with doxycycline (Dox; 30 mg/kg/day). Data normalised to GAPDH expression represent mean ± SEM (saline-infused TgNOR-1^{VSMC}, n=10; AngII-infused TgNOR-1^{VSMC}, n= 15; AngII-infused TgNOR-1^{VSMC} + doxycycline, n= 10). **B)** TH protein levels analysed by Western-blot in the same experimental groups. (Sal; open symbols, AngII; black symbols and AngII+Dox; grey symbols). Levels of β-actin are shown as a loading control. Protein size was estimated by the indicated position of molecular weight markers. The immunoblot densitometric analysis is shown in the lower panel. Data are mean ± SEM (n= 7). **P*< 0.05, ***P*< 0.01 *vs*. saline-infused mice; $^{\#}$*P*< 0.05, $^{\#\#}$*P*< 0.01 *vs*. AngII-infused TgNOR-1^{VSMC} mice non-treated with AMPT. Kruskal-Wallis test (A and B).

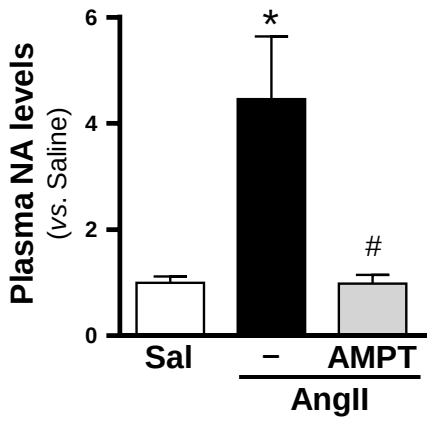

Figure S5. AMPT normalizes plasma noradrenaline levels. Circulating levels of noradrenaline (NA) were assessed by ELISA in plasma from ApoE$^{-/-}$ mice infused with saline (Sal) or AngII (1000 ng/kg/min) for 28 days. AngII-infused mice were treated or not with α-methyl-p-tyrosine (AMPT; 100 mg/Kg twice daily, i.p). Results are shown as mean ± SEM. $P<0.01$: * *vs*. saline; # *vs*. AngII-infused mice non-treated with AMPT (n=10). One-way ANOVA.

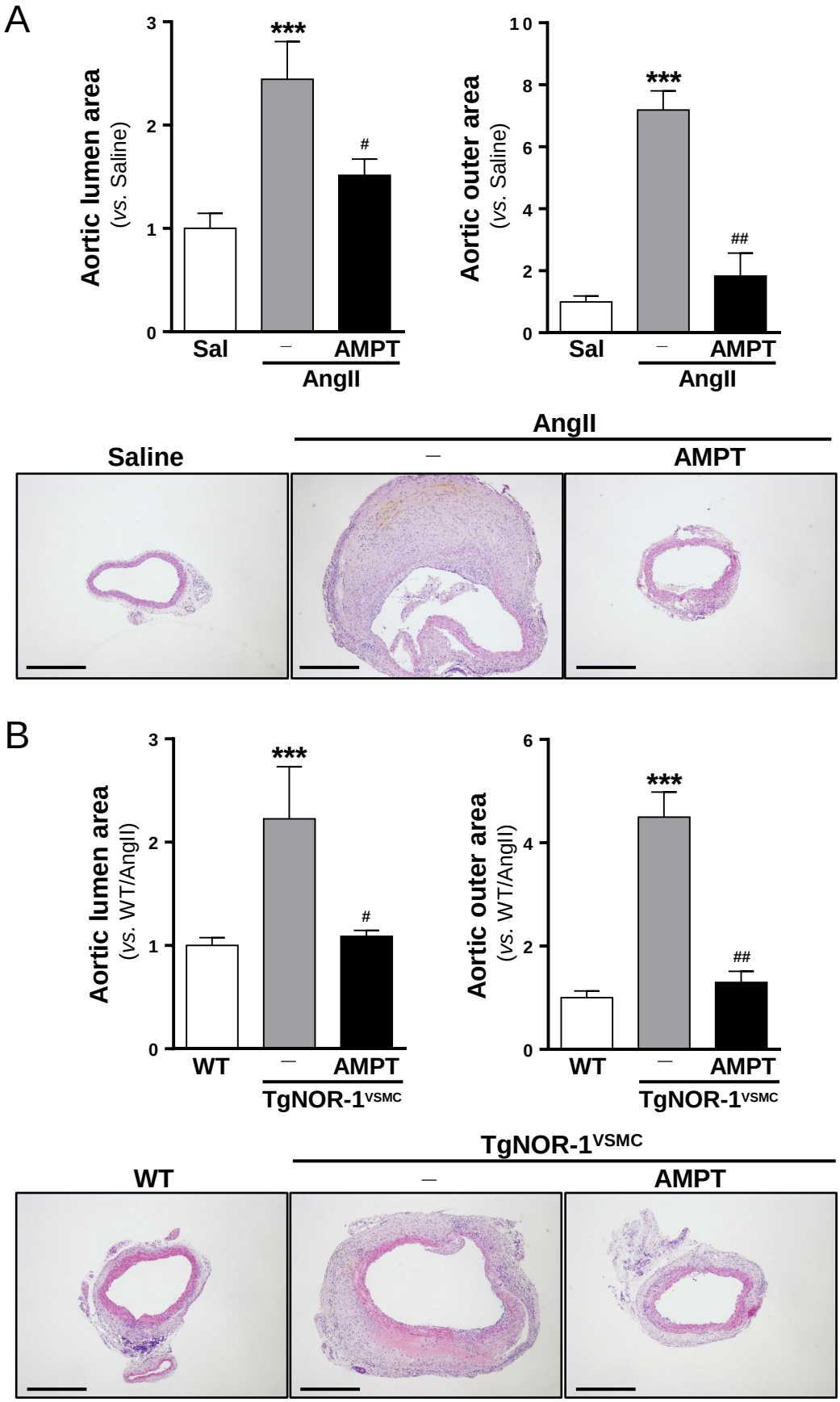

Figure S6. AMPT prevents aortic dilatation and the formation of AAA. Luminal and outer areas of abdominal aortas were quantified by image analysis in haematoxylin-stained aortic sections from **A)** ApoE$^{-/-}$ mice infused with Saline or AngII (1000 ng/kg/min, 28 days) and treated or not with α-methyl-p-tyrosine (AMPT; 100 mg/Kg twice daily, i.p) and **B)** WT and TgNOR-1^{VSMC} infused with AngII for 28 days. AngII-infused TgNOR-1^{VSMC} were treated or not with AMPT. (WT: wild-type; Tg^{VSMC}: TgNOR-1^{VSMC} animals). Data represent mean ± SEM (n=10). ***P< 0.001 *vs.* saline-infused ApoE$^{-/-}$ mice or AngII-infused WT mice; $^{\#}P$< 0.05, $^{\#\#}P$< 0.01 *vs.* AngII-infused mice non-treated with AMPT. Kruskal-Wallis (A) or One-way ANOVA (B) tests. Haematoxylin-stained sections of abdominal aortas are shown in lower panels (Bars: 500 µm).

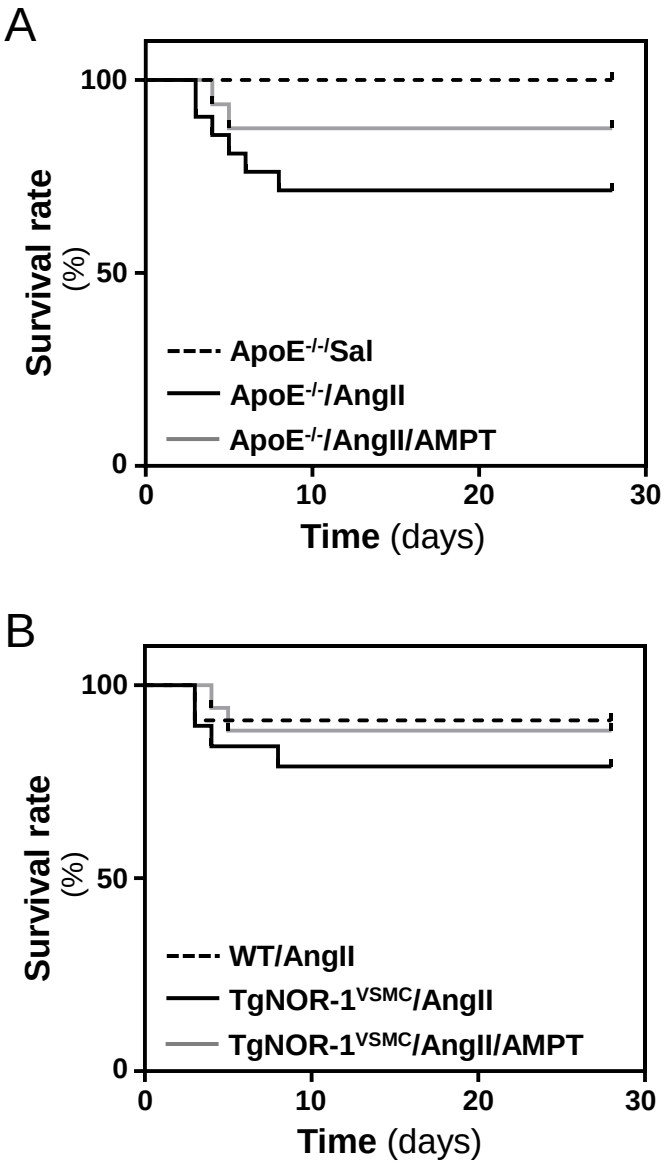

Figure S7. Graph showing the survival rate in the two mouse models. A) ApoE$^{-/-}$ mice were infused with saline (Sal) or AngII (1000 ng/kg/min) for 28 days. AngII-infused ApoE$^{-/-}$ mice were treated or not with α-methyl-p-tyrosine (AMPT; 100 mg/Kg twice daily, i.p). The graph shows the survival rate of each experimental group (saline-infused ApoE$^{-/-}$ mice, n= 9; AngII-infused ApoE$^{-/-}$ mice, n= 21 [6 deaths]; AngII-infused ApoE$^{-/-}$ mice treated with AMPT, n= 17 [2 deaths]). **B)** Graph showing the survival rate of wild-type (WT) and TgNOR-1^{VSMC} mice both infused with AngII (1000 ng/kg/min) for 28 days. TgNOR-1^{VSMC} mice were treated or not with AMPT (WT, n= 11 [1 death]; TgNOR-1^{VSMC} non-treated with AMPT, n= 19 [4 deaths]; TgNOR-1^{VSMC} treated with AMPT, n= 17 [2 deaths]). There were no deaths in saline-infused groups (not shown). Chi-square test.

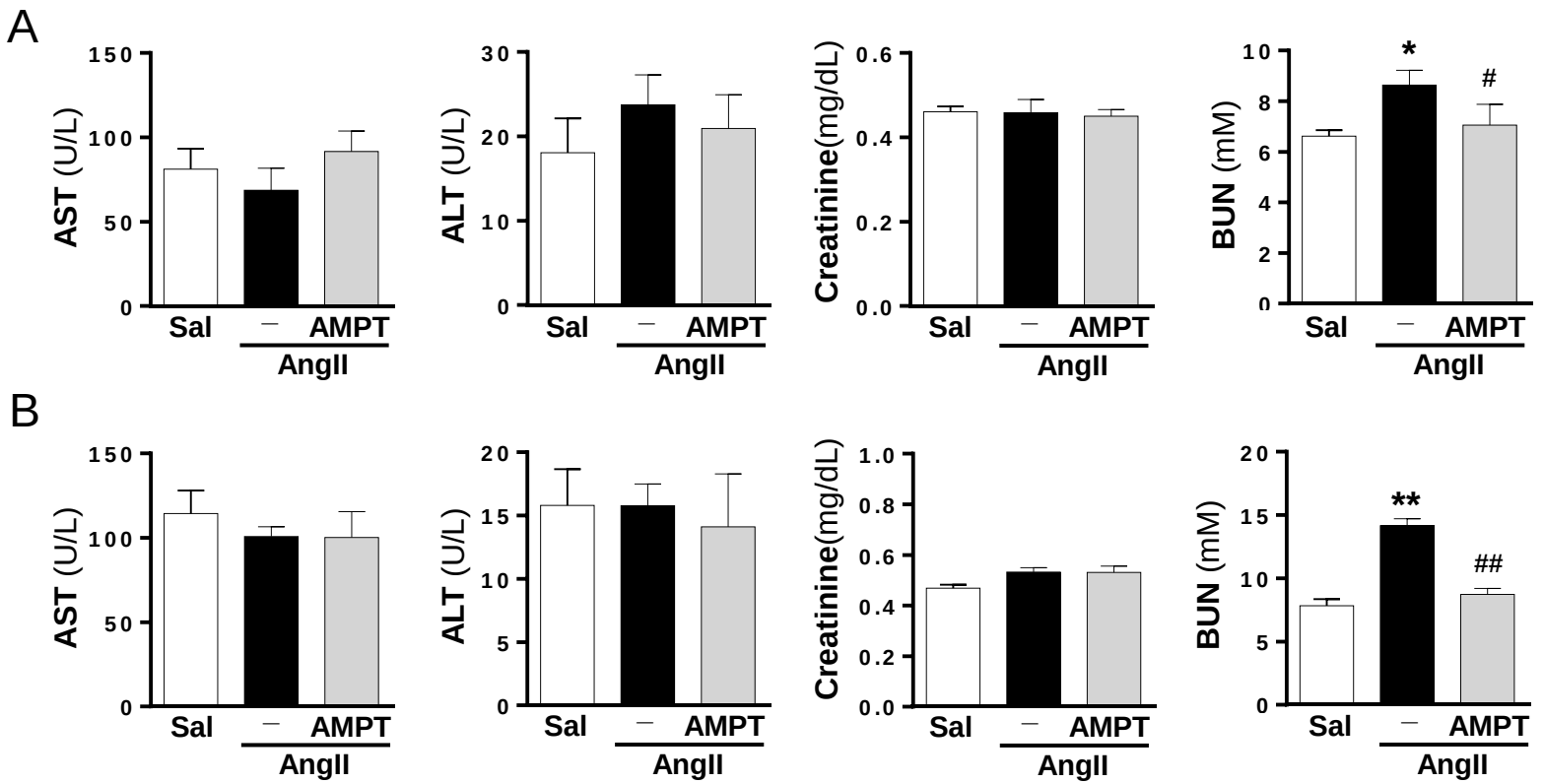

Figure S8. **Impact of AMPT on renal and hepatic function in AngII-infused ApoE$^{-/-}$ and TgNOR-1^{VSMC} mice.** Biochemical parameters of renal and hepatic function were assessed in plasma samples from ApoE$^{-/-}$ (**A**) and TgNOR-1^{VSMC} (**B**) mice infused with saline (Sal) or AngII (treated or not with α-methyl-p-tyrosine [AMPT; 100 mg/Kg twice daily, i.p]). Levels of aspartate transaminase (AST) alanine transaminase (ALT), creatinine and blood urea nitrogen (BUN) are shown. Data represent mean ± SEM (ApoE$^{-/-}$ saline, n=10; ApoE$^{-/-}$ AngII, n=11; ApoE$^{-/-}$ AngII + AMPT, n=10; TgNOR-1^{VSMC} saline, n=9; AngII-infused TgNOR-1^{VSMC} treated or not with AMPT, n=11). *P< 0.05, **P< 0.001 *vs*. saline-infused mice; $^{\#}P$< 0.05, $^{\#\#}P$< 0.001 *vs*. AngII-infused mice non-treated with AMPT. Kruskal-Wallis test (A and B).

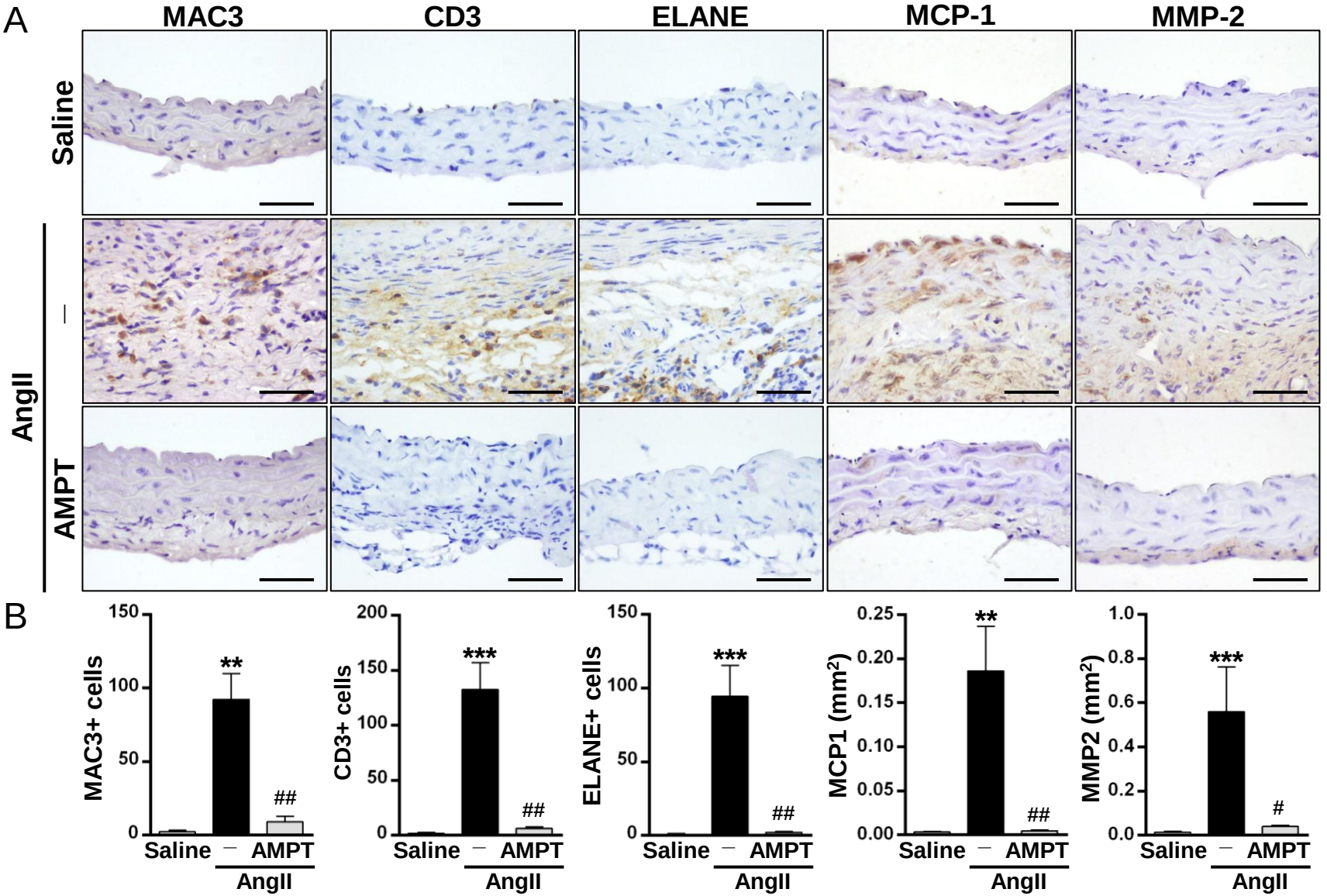

Figure S9. Inflammation and MMP2 levels were attenuated by AMPT in the abdominal aorta from AngII-infused ApoE$^{-/-}$ mice. ApoE$^{-/-}$ mice were infused with saline or AngII (1000 ng/kg/min) for 28 days. AngII-infused mice were left untreated or treated with α-methyl-*p*-tyrosine (AMPT; 100 mg/Kg twice daily, i.p). **A)** Aortic infiltration of macrophages (MAC3), lymphocytes (CD3) and neutrophils (elastase, neutrophil expressed, ELANE) and staining for MCP1 and MMP2 in each group (Bars: 50 µm). **B)** Quantitative analysis of positive cells *per* aortic section (MAC3, CD3 and ELANE) and area in mm^2 *per* aortic section (MCP1 and MMP2). Data are expressed as mean ± SEM (saline, n= 6; AngII-infused groups, n=9). ***P*< 0.01, ****P*< 0.001 *vs.* Saline-infused ApoE$^{-/-}$ mice; $^{\#}$*P*< 0.05, $^{\#\#}$*P*< 0.01 *vs*. AngII-infused ApoE$^{-/-}$ mice non-treated with AMPT. Kruskal–Wallis test.

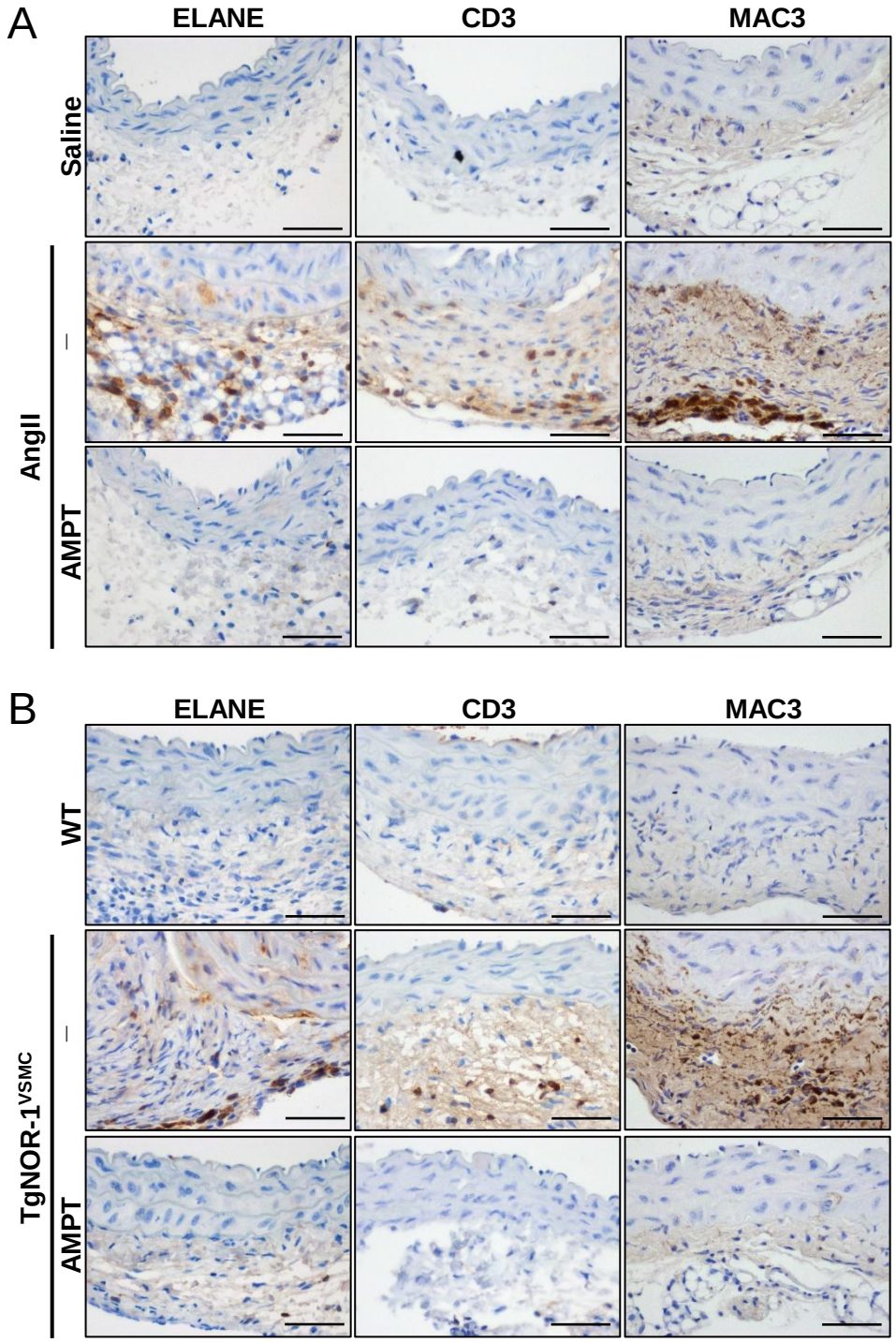

Figure S10. Inflammation was attenuated by AMPT in experimental mouse models of AAA. Representative images of aortic infiltration of neutrophils (elastase, neutrophil expressed, ELANE), lymphocytes (CD3) and macrophages (MAC3) in abdominal aortas from **A)** ApoE$^{-/-}$ mice infused with Saline or AngII (1000 ng/kg/min, 28 days) and treated or not with α-methyl-p-tyrosine (AMPT; 100 mg/Kg twice daily, i.p) and **B)** WT and TgNOR-1^{VSMC} infused with AngII for 28 days. AngII-infused TgNOR-1^{VSMC} were treated or not with AMPT. (WT: wild-type). The anti-inflammatory effect of AMPT was also evident in samples containing perivascular fat (with intact adventitia).

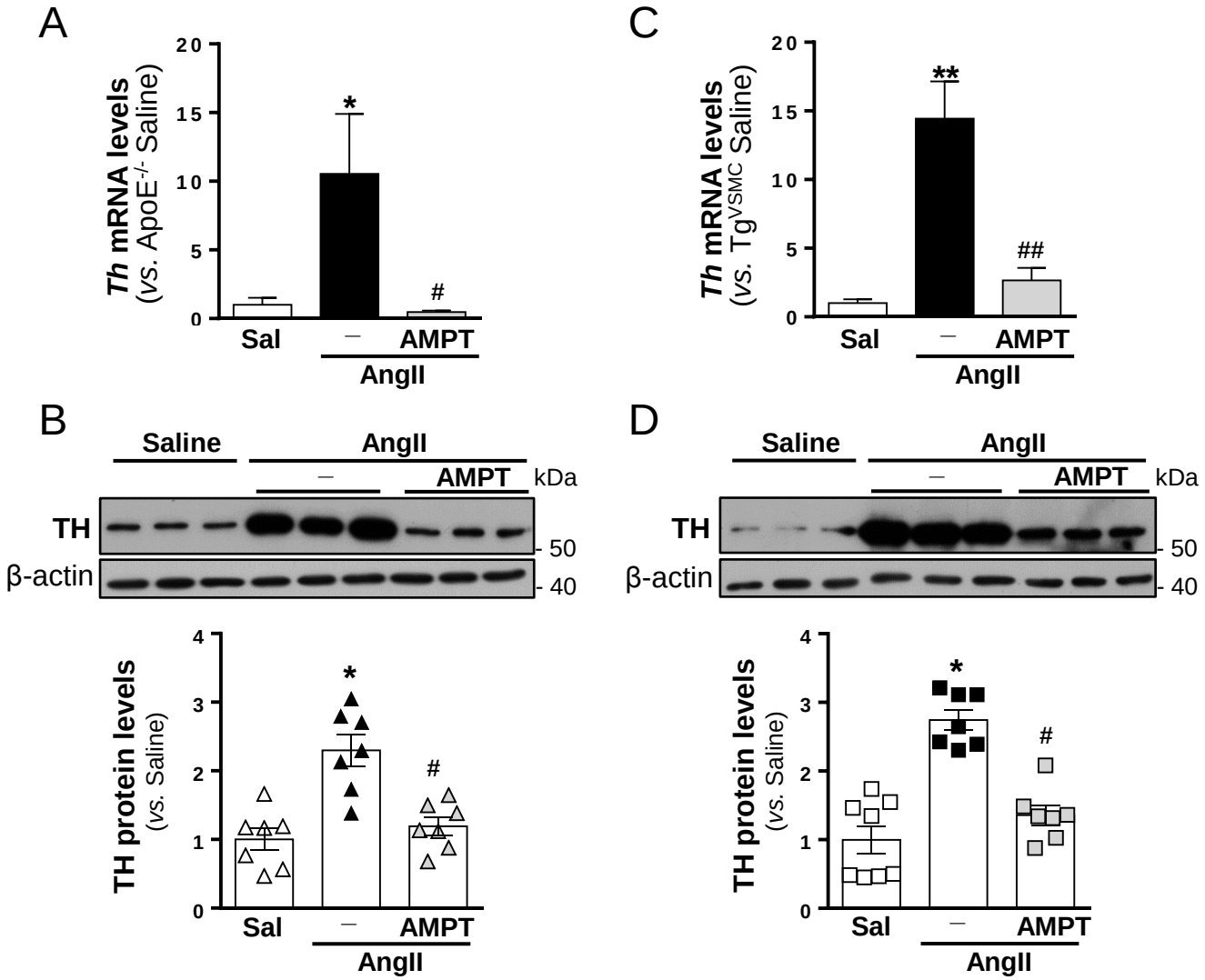

Figure S11. AMPT prevents the increase in aortic TH expression induced by AngII-infusion in experimental mouse models of AAA. A and **C)** *Th* mRNA levels were analysed by real-time PCR in abdominal aorta samples from ApoE$^{-/-}$ (**A**) or TgNOR-1^{VSMC} mice (**C**) infused with saline (Sal) or AngII (1000 ng/kg/min for 28 days), treated or not with α-methyl-p-tyrosine (AMPT; 100 mg/Kg twice daily, i.p). Data normalised to GAPDH expression represent mean ± SEM (saline-infused ApoE$^{-/-}$ mice, n= 9; AngII-infused ApoE$^{-/-}$ mice treated or not with AMPT, n= 10; saline-infused TgNOR-1^{VSMC}, n= 10; AngII-infused TgNOR-1^{VSMC} treated or not with AMPT, n= 15). **B** and **D**) Aortic TH protein levels were assessed by Western-blot in samples from ApoE$^{-/-}$ (B) and TgNOR-1^{VSMC} (D) mice treated as described above (Sal; open symbols, AngII; black symbols and AngII+AMPT; grey symbols). Levels of β-actin are shown as a loading control. Protein size was estimated by the indicated position of molecular weight markers. Immunoblots densitometric analysis are shown in the lower panels. Data are mean ± SEM (n= 7). *P< 0.05, **P< 0.001 *vs*. saline-infused mice; $^{\#}P$< 0.05, $^{\#\#}P$< 0.001 *vs.* AngII-infused mice non-treated with AMPT. Kruskal-Wallis (A-D).

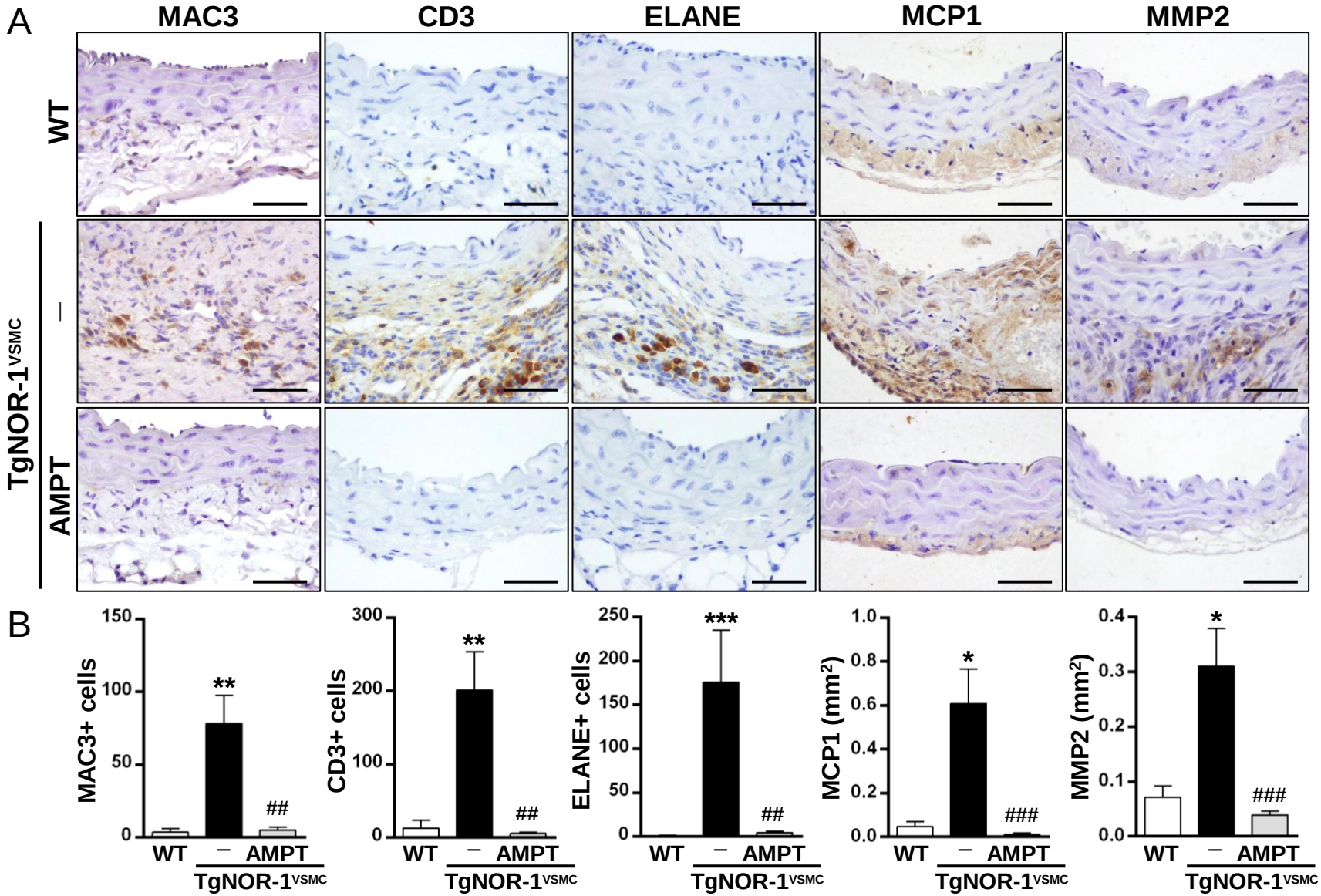

Figure S12. AMPT attenuates inflammation and MMP2 expression in the abdominal aorta from AngII-infused TgNOR-1^{VSMC} mice. Wild-type (WT) and TgNOR-1^{VSMC} mice were infused with AngII (1000 ng/kg/min; 28 days). TgNOR-1^{VSMC} mice were treated or not with α-methyl-*p*-tyrosine (AMPT; 100 mg/Kg twice daily, i.p). **A)** Infiltration of macrophages (MAC3), lymphocytes (CD3) and neutrophils (elastase, neutrophil expressed, ELANE) and staining for MCP1 and MMP2 (Bars: 50 μm). **B)** Positive cells *per* aortic section (MAC3, CD3 and ELANE) and area in mm^2 *per* aortic section (MCP1 and MMP2). Data are mean ± SEM (WT, n= 6; TgNOR-1^{VSMC}, n=8; TgNOR-1^{VSMC} + AMPT, n=10). **P*< 0.05, ***P*< 0.01, ****P*< 0.001 *vs.* WT; $^{\#\#}$*P*< 0.01, $^{\#\#\#}$*P*< 0.001 *vs.* TgNOR-1^{VSMC} non-treated with AMPT. Kruskal–Wallis test.

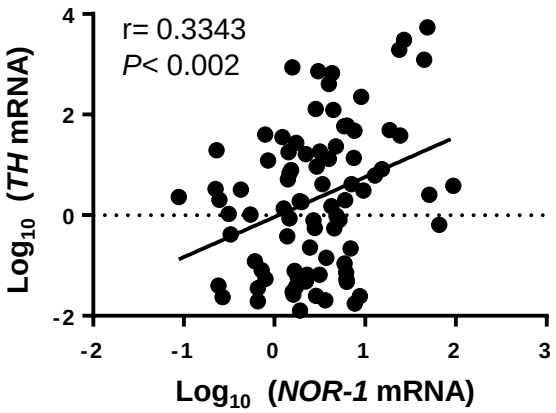

Figure S13. Vascular expression of *NOR-1* correlates with that of *TH* in human AAA. Statistically significant positive correlation between NOR-1 mRNA levels and those corresponding to tyrosine hydroxylase (*TH)* in aneurysmal samples from AAA patients (n= 84). The Pearson Product Moment Correlation was applied.

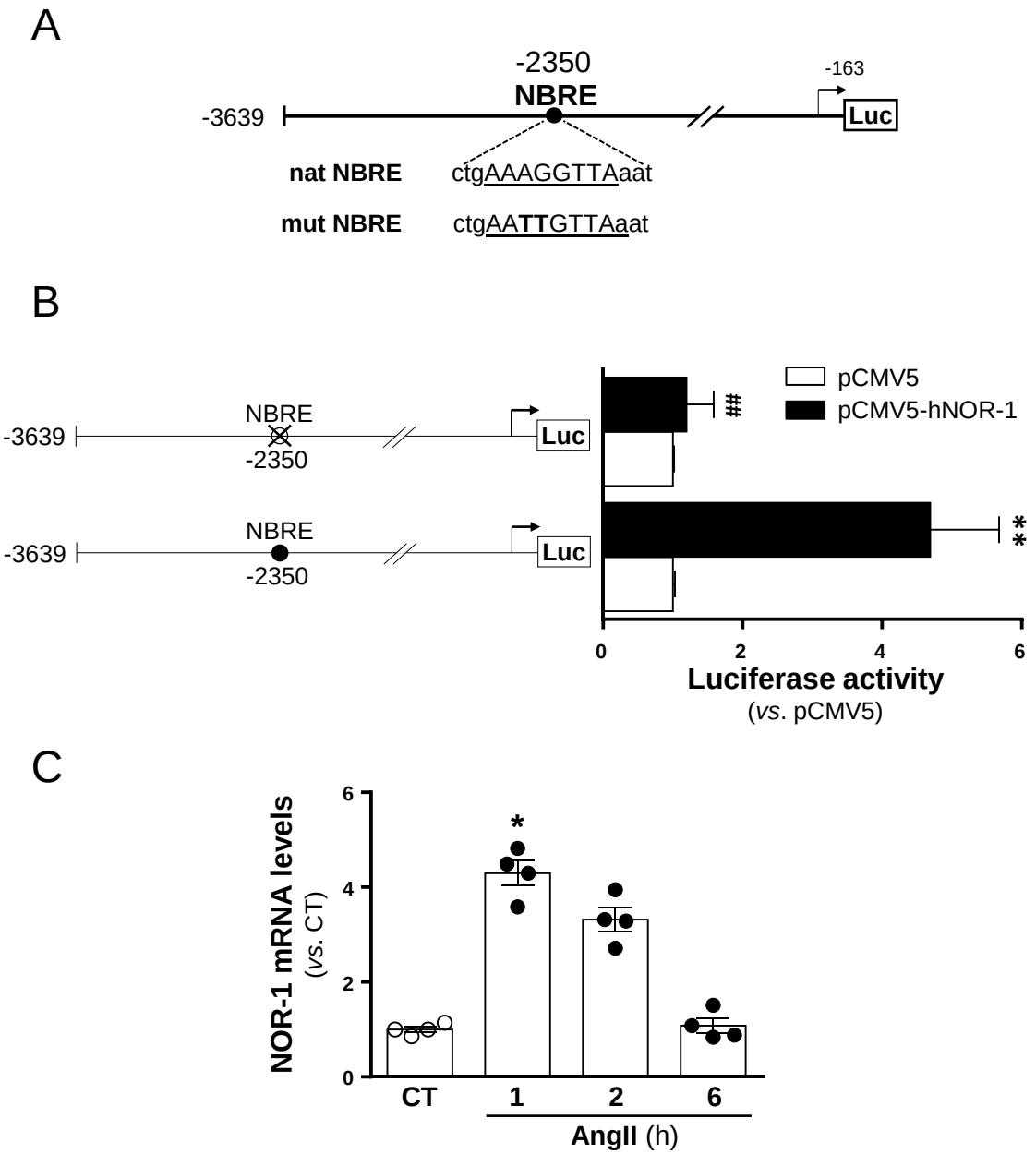

Figure S14. NOR-1 regulates tyrosine hydroxylase (*TH*) transcriptional activity. A) Scheme depicting the structure of the proximal region of the human *TH* promoter and the location and sequence of the putative NBRE identified *in silico*. The native NBRE (nat NBRE) and the corresponding mutated sequence (mut NBRE) are underlined. Changes introduced by mutagenesis are highlighted in bold. **B)** Luciferase activity evaluated in rat vascular smooth muscle cells co-transfected with the luciferase reporter construct pGL3/pTH–3639 (or the form mutated in the putative NBRE located at -2350 bp) and a NOR-1 expression vector (pCMV5-NOR-1; black bars) or the corresponding empty plasmid (pCMV5; white bars). Data were normalised by Renilla luciferase activity and expressed as mean ± SEM (n= 8).***P*< 0.0001 *vs*. control cells or cells cotransfected with pCMV5; $^{\#\#}P$< 0.0001 *vs*. cells cotransfected with the native pGL3/pTH–3639 and pCMV5-NOR-1 plasmids. **C)** NOR-1 mRNA levels assessed by real-time PCR in mouse VSMC exposed to AngII (10^{-7} M) for the indicated times (CT; open symbols, AngII-treated cells; filled symbols). Results are shown as mean ± SEM. **P*< 0.05 *vs*. CT (n=4). Two-way ANOVA (B) and Kruskal Wallis test (C).

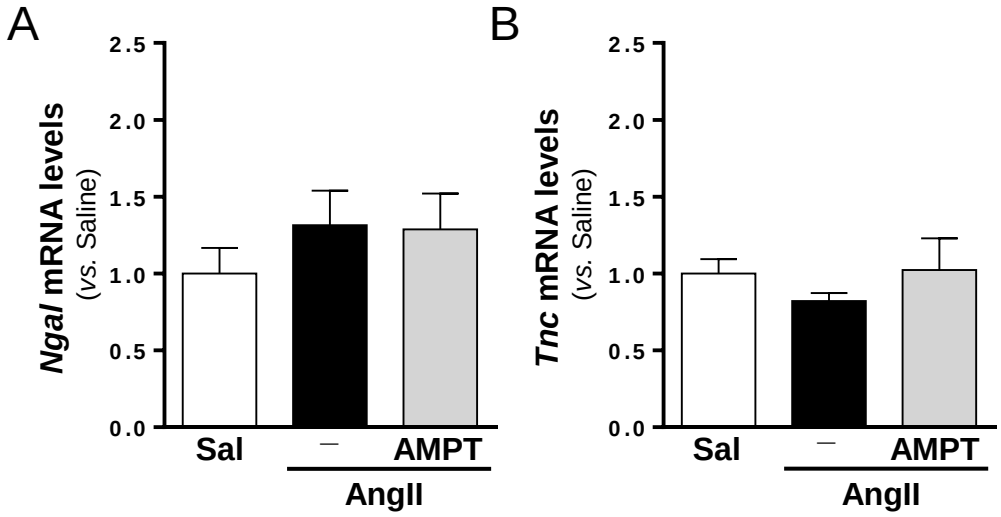

Figure S15: AngII-infusion did not alter the renal expression of markers of renal damage. mRNA levels of *Ngal* (**A**) and *Tnc* (**B**) were assessed by real-time PCR in kidneys from ApoE$^{-/-}$ mice infused with saline (Sal) or AngII (1000 ng/kg/min; 28 days), treated or not with α-methyl-p-tyrosine (AMPT; 100 mg/Kg twice daily, i.p). Results are shown as mean ± SEM (AngII-infused animals non-treated with AMPT n=8; AngII-infused mice treated with AMPT, n=7; Saline, n=5). Kruskal-Wallis test

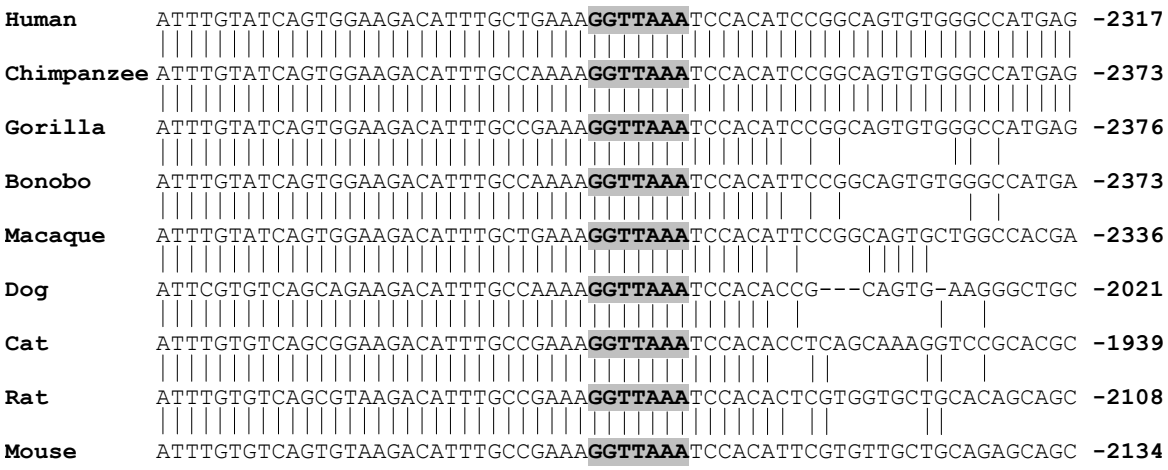

Figure S16. **The NBRE site in *TH* promoter is conserved among species.** *TH* promoter sequence surrounding the putative NBRE site located at -2350 bp in human *TH* gene (ENSG00000180176) was aligned with those from different species using Blast program. The conserved bases are indicated and the NBRE site in each sequence is highlighted in grey.